12

DAHLGREN DIVISION
NAVAL SURFACE WARFARE CENTER
Panama City, Florida 32407-7001

CSS/TR-94/32

COMPLETE ANALYSIS OF ELECTRODE-TERMINATED CABLES IN TWO-LAYER CONDUCTOR BOUNDED ABOVE BY AIR: CURRENT DENSITY, MAGNETIC FIELD, AND MAGNETIC FIELD GRADIENT

BY W. M. WYNN

COASTAL RESEARCH AND TECHNOLOGY DEPARTMENT

DECEMBER 1994

15

Coastal Systems Station, Dahlgren Division
Naval Surface Warfare Center
PANAMA CITY, FLORIDA 32407-7001

CAPT D. C. STEERE, USN
Commanding Officer

MR. TED C. BUCKLEY
Executive Director

ADMINISTRATIVE INFORMATION

This work was done under various funding sources over a period of several years. The sources include Coastal Systems Station, Dahlgren Division, Naval Surface Warfare Center, Panama City, Florida, Independent Exploratory Development, multi-agency consulting, and for the final improvements and reporting, the Office of Naval Research under *Environmental Physics for Mine Countermeasures (MCM), Task 3 (R035P03), MCM Geomagnetic and Geoelectric Environment.*

Released by
D. P. SKINNER, Head
Coastal Research and
Technology Department

Under authority of
T. C. BUCKLEY
Executive Director

REPORT DOCUMENTATION PAGE

Form Approved
OBM No. 0704-0188

1. AGENCY USE ONLY (*Leave blank*)

2. REPORT DATE
December 1994

3. REPORT TYPE AND DATES COVERED

4. TITLE AND SUBTITLE
Complete Analysis of Electrode-Terminated Cables in Two-Layer Conductor Bounded Above by Air: Current Density, Magnetic Field, and Magnetic Field Gradient

5. FUNDING NUMBERS

6. AUTHOR(s)
W. M. Wynn

7. PERFORMING ORGANIZATION NAME(S) AND ADDRESS(ES)
Attn: Code 110
Commanding Officer
CSSDD NSWC
6703 West Highway 98
Panama City, FL 32407-7001

8. PERFORMING ORGANIZATION REPORT NUMBER
CSS/TR-94/32

9. SPONSORING/MONITORING AGENCY NAME(S) AND ADDRESS(ES)

10. SPONSORING/MONITORING AGENCY REPORT NUMBER

11. SUPPLEMENTARY NOTES

12a. DISTRIBUTION/AVAILABILITY STATEMENT
Approved for public release; distribution is unlimited.

12b. DISTRIBUTION CODE

13. ABSTRACT (*Maximum 200 words*)

A complete analysis is given for the current density, magnetic field, and magnetic field gradient of a point current source located in the upper layer of a two-layer conductor that is bounded above by air. This problem has a long history, and treatments of varying degrees of completeness and/or rigor are scattered throughout the older geophysical literature. The intent here is to do a complete, self-contained analysis based on potential theory and Ampere's Law; treat all possible cases for the relative conductivity of the media, including the special cases of a lower medium that is an insulator or a perfect conductor; and provide expressions for the magnetic field vector, the current density vector, and the magnetic field gradient tensor in both conducting layers. The effect of performing gradient measurements within an enclosure also is discussed. The principle new results are the inclusion of expressions for the current density and magnetic field in the lower conducting layer, expressions for the magnetic field gradient tensor in both conducting layers, and the analysis of the case of a perfectly conducting lower layer. To complete the set of tools needed to describe a cable terminated by point electrodes, compact general expressions are given for the magnetic field vector and magnetic gradient tensor for a straight current element with arbitrary end points. These are based on the Biot-Savart Law and can be used to calculate the field and gradient contribution from an arbitrary cable joining two or more electrodes by means of superposition. The end results are applicable to such diverse problems as long-wire, electro-prospecting the current distribution around sheet piling protected by active electrodes, and the distributed currents of grounded direct current power systems.

14. SUBJECT TERMS
Electrode; Cable; Two-Layer Conductor; Magnetic Field; Current Density; Magnetic Field Gradient; Biot-Savart Field; Biot-Savart Gradient; Electrode Field; Electrode Gradient

15. NUMBER OF PAGES
49

16. PRICE CODE

17. SECURITY CLASSIFICATION OF REPORT	18. SECURITY CLASSIFICATION OF THIS PAGE	19. SECURITY CLASSIFICATION OF ABSTRACT	20. LIMITATION OF ABSTRACT
UNCLASSIFIED	UNCLASSIFIED	UNCLASSIFIED	UL

NSN 7540-01-280-5500

Standard Form 298 (Rev 2-89)
Prescribed by ANSI std. Z39-18
298-102

CONTENTS

ILLUSTRATIONS

INTRODUCTION

The geometry for the following analysis is shown in Figure 1. A point source of current I is located on the z axis at z coordinate h. Space is divided into three regions with electrical conductivities as follows:

$$\sigma = 0\,, -\infty < z \leq 0 \quad \text{(region 0)} \tag{1a}$$

$$\sigma = \sigma_1\,, 0 < z \leq d \quad \text{(region 1)} \tag{1b}$$

$$\sigma = \sigma_2\,, d < z < \infty \quad \text{(region 2)} \tag{1c}$$

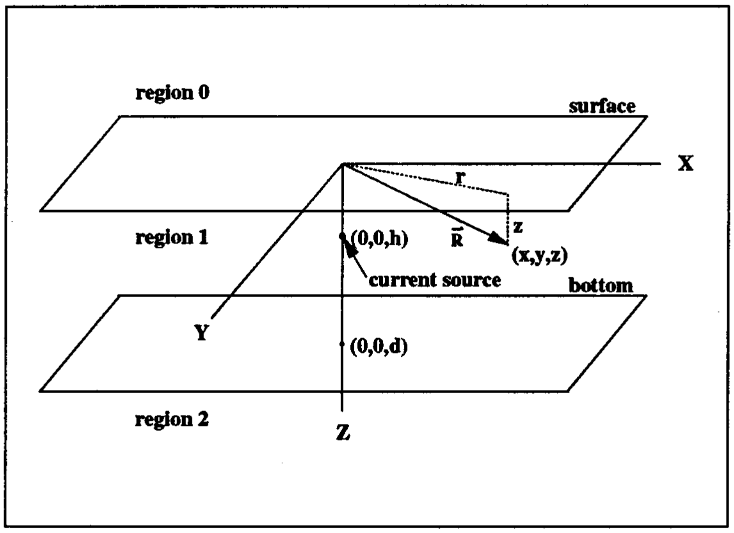

FIGURE 1. GEOMETRY FOR POINT CURRENT SOURCE FIELDS

The source is located in the middle region. It has a potential of the form

$$\Phi_P = \frac{I}{4\pi\sigma_1\sqrt{r^2 + (z-h)^2}}, \tag{2}$$

which has the integral representation

$$\Phi_P = \frac{I}{4\pi\sigma_1}\int_0^\infty d\lambda J_0(\lambda r)e^{-\lambda|z-h|}. \tag{3}$$

Elsewhere, the potential function satisfies Laplace's equation

$$\nabla^2\Phi(r,\theta,z) = 0, \tag{4}$$

which has the axially symmetric solution in cylindrical coordinates

$$\Phi_H = \int_0^\infty d\lambda J_0(\lambda r)\,[a(\lambda)e^{\lambda z} + b(\lambda)e^{-\lambda z}]. \tag{5}$$

The potential in the three regions then has the physically acceptable forms

$$\Phi_0 = \int_0^\infty d\lambda J_0(\lambda r) a_0(\lambda) e^{\lambda z} \quad (-\infty < z \le 0) \tag{6}$$

$$\Phi_1 = \int_0^\infty d\lambda J_0(\lambda r)\left[\frac{I}{4\pi\sigma_1} e^{-\lambda|z-h|} + a_1(\lambda)e^{\lambda z} + b_1(\lambda)e^{-\lambda z}\right] \quad (0 < z \le d) \tag{7}$$

and

$$\Phi_2 = \int_0^\infty J_0(\lambda r) b_2(\lambda) e^{-\lambda z} \quad (d < z < \infty). \tag{8}$$

BOUNDARY CONDITIONS

The boundary conditions require continuity of the normal component of the current density and the tangential component of the electric field at each boundary. The electric field and current density are given by

$$\mathbf{E} = -\nabla\Phi \quad \text{and} \quad \mathbf{J} = \sigma\mathbf{E}. \tag{9}$$

Continuity of the normal current density at each boundary leads to the equations

$$a_1(\lambda) - b_1(\lambda) = -\frac{I}{4\pi\sigma_1} e^{-\lambda h} \tag{10}$$

and

$$a_1(\lambda)e^{\lambda d} - b_1(\lambda)e^{-\lambda d} + \varepsilon b_2(\lambda)e^{-\lambda d} = \frac{I}{4\pi\sigma_1} e^{-\lambda(d-h)} \tag{11}$$

where

$$\varepsilon = \sigma_2/\sigma_1. \tag{12}$$

Continuity of the tangential electric field at the bottom gives the equation

$$a_1(\lambda)e^{\lambda d} + b_1(\lambda)e^{-\lambda d} - b_2(\lambda)e^{-\lambda d} = \frac{I}{4\pi\sigma_1} e^{-\lambda(d-h)}. \tag{13}$$

Equations (11) ,(12), and (13) are sufficient to determine $a_1(\lambda)$, $b_1(\lambda)$, and $b_2(\lambda)$. This allows the computation of all fields in the middle and lower regions, which are of primary interest here. The function $a_0(\lambda)$ can be determined from continuity of the tangential electric field at the air-conductor interface, if needed.

With the introduction of the parameter $Q = (1-\varepsilon)/(1+\varepsilon)$, the solutions for the coefficients in the upper and lower conducting regions can be written

$$a_1(\lambda) = \frac{I}{4\pi\sigma_1}\frac{Qe^{-2\lambda d}}{1-Qe^{-2\lambda d}}(e^{\lambda h}+e^{-\lambda h}) \tag{14}$$

$$b_1(\lambda) = \frac{I}{4\pi\sigma_1}\left[e^{-\lambda h}+\frac{Qe^{-2\lambda d}}{1-Qe^{-2\lambda d}}(e^{\lambda h}+e^{-\lambda h})\right] \tag{15}$$

and

$$b_2(\lambda) = \frac{I}{4\pi\sigma_2}\frac{(1-Q)(e^{\lambda h}+e^{-\lambda h})}{1-Qe^{-2\lambda d}}. \tag{16}$$

The parameter Q has the range of values $-1 \le Q \le 1$, where $Q = 1$ corresponds to region 2 being a perfect insulator, $Q = 0$ corresponds to regions 1 and 2 being identical, and $Q = -1$ corresponds to region 2 being a perfect conductor.

POTENTIAL AND CURRENT DENSITY

The potential for the middle and lower regions is given by

$$\Phi_1 = \frac{I}{4\pi\sigma_1}\int_0^\infty d\lambda J_0(\lambda r)\{e^{-\lambda|z-h|}+e^{-\lambda(z+h)} \tag{17}$$

$$+\frac{Qe^{-2\lambda d}}{1-Qe^{-2\lambda d}}[e^{\lambda(z+h)}+e^{-\lambda(z+h)}+e^{\lambda(z-h)}+e^{-\lambda(z-h)}]\}$$

and

$$\Phi_2 = \frac{I}{4\pi\sigma_2}(1-Q)\int_0^\infty d\lambda J_0(\lambda r)\left[\frac{e^{-\lambda(z-h)}+e^{-\lambda(z+h)}}{1-Qe^{-2\lambda d}}\right]. \tag{18}$$

Integrals involving the bessel functions are notoriously difficult to perform numerically. However, a geometric series expansion valid for $|Q| < 1$

$$\frac{1}{1-Qe^{-2\lambda d}} = \sum_{n=0}^{\infty} Q^n e^{-2n\lambda d} \tag{19}$$

and the integral representations exemplified by Equations (2) and (3) can be used to write the potential in the upper and lower conductors as

$$\Phi_1=\frac{I}{4\pi\sigma_1}\{\frac{1}{\sqrt{r^2+(z-h)^2}}+\frac{1}{\sqrt{r^2+(z+h)^2}}+\sum_{n=1}^{\infty}Q^n[\frac{1}{\sqrt{r^2+(2nd-z-h)^2}} \tag{20}$$

$$+\frac{1}{\sqrt{r^2+(2nd+z+h)^2}}+\frac{1}{\sqrt{r^2+(2nd-z+h)^2}}+\frac{1}{\sqrt{r^2+(2nd+z-h)^2}}]\}$$

and

$$\Phi_2=\frac{I}{4\pi\sigma_2}(1-Q)\{\frac{1}{\sqrt{r^2+(z-h)^2}}+\frac{1}{\sqrt{r^2+(z+h)^2}} \tag{21}$$

$$+\sum_{n=1}^{\infty}Q^n\left[\frac{1}{\sqrt{r^2+(2nd+z-h)^2}}+\frac{1}{\sqrt{r^2+(2nd+z+h)^2}}\right]\}.$$

By combining Equation (9) with Equations (20) and (21), expressions for the cartesian components of the current density in the middle and lower regions can be derived. They are

$$J_{1x(y)}=\frac{x(y)I}{4\pi}\{\frac{1}{\sqrt{(r^2+(z-h)^2)^3}}+\frac{1}{\sqrt{(r^2+(z+h)^2)^3}}+\sum_{n=1}^{\infty}Q^n[\frac{1}{\sqrt{(r^2+(2nd-z-h)^2)^3}} \tag{22}$$

$$+\frac{1}{\sqrt{(r^2+(2nd+z+h)^2)^3}}+\frac{1}{\sqrt{(r^2+(2nd-z+h)^2)^3}}+\frac{1}{\sqrt{(r^2+(2nd+z-h)^2)^3}}]\}$$

$$J_{1z}=\frac{I}{4\pi}\{\frac{|z-h|}{\sqrt{(r^2+(z-h)^2)^3}}+\frac{z+h}{\sqrt{(r^2+(z+h)^2)^3}}+\sum_{n=1}^{\infty}Q^n[-\frac{2nd-z-h}{\sqrt{(r^2+(2nd-z-h)^2)^3}} \tag{23}$$

$$+\frac{2nd+z+h}{\sqrt{(r^2+(2nd+z+h)^2)^3}}-\frac{2nd-z+h}{\sqrt{(r^2+(2nd-z+h)^2)^3}}+\frac{2nd+z-h}{\sqrt{(r^2+(2nd+z-h)^2)^3}}]\}.$$

$$J_{2x(y)}=\frac{x(y)I}{4\pi}(1-Q)\sum_{n=0}^{\infty}Q^n\left[\frac{1}{\sqrt{(r^2+(2nd+z-h)^2)^3}}+\frac{1}{\sqrt{(r^2+(2nd+z+h)^2)^3}}\right] \tag{24}$$

and

$$J_{2z}=\frac{I}{4\pi}(1-Q)\sum_{n=0}^{\infty}Q^n\left[\frac{2nd+z-h}{\sqrt{(r^2+(2nd+z-h)^2)^3}}+\frac{2nd+z+h}{\sqrt{(r^2+(2nd+z+h)^2)^3}}\right] \tag{25}$$

MAGNETIC FIELD DUE TO DISTRIBUTED CURRENT

The magnetic field of the distributed current can be constructed by means of a careful application of Ampere's Law, applied to a properly constructed system; that is, one in which charge conservation holds. To accomplish this, the point current source is imagined to be fed by an insulated wire that enters region 1 perpendicular to the boundaries, and extends into medium 0 for a great distance, ultimately returning to a point current sink in region 1 at a great lateral distance from the current source. Application of the Biot-Savart Law to the wire shows that if the wire extends far enough from the boundary in the z direction and returns to the medium sufficiently far away, the magnetic field of the wire segment is indistinguishable from that of a semi-infinite wire extending in the $-z$ direction. In addition, if the current sink is sufficiently far away, its fields are negligible at the current source, and axial symmetry about the incoming wire can be applied. This is illustrated in Figure 2.

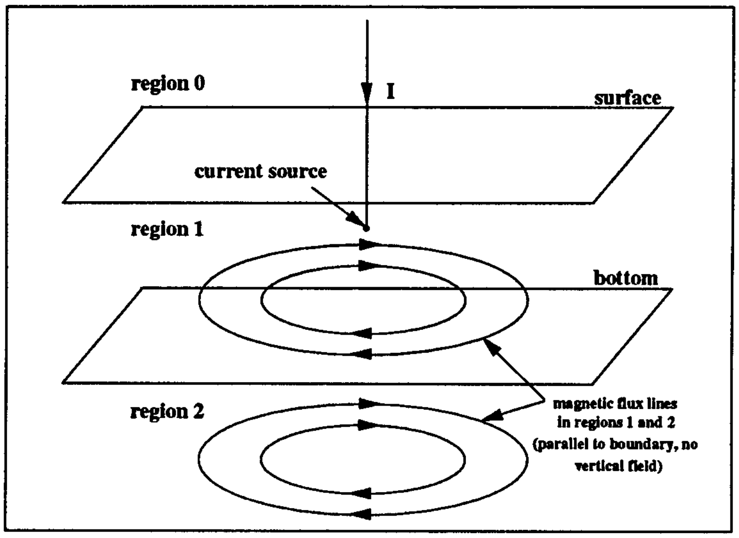

FIGURE 2. MAGNETIC FIELD OF WIRE AND DISTRIBUTED CURRENTS*

Ampere's Law can now be applied to the current distribution. Ampere's Law takes the form

$$\oint \mathbf{H} \cdot d\mathbf{l} = \int \mathbf{J} \cdot d\mathbf{A}, \tag{26}$$

which states that the line integral of the magnetic field around a closed path is equal to the integral of the normal current density over the enclosed surface; that is, the net current through the loop. In the present application, symmetry about the wire axis can be used to write

$$\oint \mathbf{H} \cdot d\mathbf{l} = 2\pi r H_\theta \tag{27}$$

*Note that the magnetic field is *entirely horizontal, there is no vertical field from the wire current or the distributed currents from the point source.*

where r is the radius of a circle centered on the wire axis and H_θ is the tangential component of magnetic field on the circle, which is the same everywhere, independent of θ. Now, if the integral on the right hand side of Equation (26) can be evaluated, the magnetic field in regions 1 and 2 can be determined directly . To accomplish this, region 2 , $d \le z < \infty$, is first examined, with reference to the notation of Figure 1. The right-hand rule is used to assign the sense of the currents and fields, and then

$$\int \mathbf{J}_2 \cdot d\mathbf{A} = \int J_{2z} dA = \int_0^{2\pi} d\theta \int_0^r du\, u J_{2z} = 2\pi \int_0^r du\, u J_{2z} \tag{28}$$

where J_{2z} is independent of θ.

Substitution of Equation (25) into Equation (28) and application of Equations (26) and (27) yields

$$H_{2\theta} = \frac{I}{4\pi r}\{2-(1-Q)(\frac{z-h}{\sqrt{r^2+(z-h)^2}}+\frac{z+h}{\sqrt{r^2+(z+h)^2}} \tag{29}$$

$$+\sum_{n=1}^{\infty} Q^n\left[\frac{2nd+z-h}{\sqrt{r^2+(2nd+z-h)^2}}+\frac{2nd+z+h}{\sqrt{r^2+(2nd+z+h)^2}}\right])\}.$$

$$(d \le z < \infty)$$

Repeating this analysis for region 1, for $h < z \le d$, and using Equation (23) instead of Equation (25),

$$H_{1\theta} = \frac{I}{4\pi r}\{2-\frac{z-h}{\sqrt{r^2+(z-h)^2}}-\frac{z+h}{\sqrt{r^2+(z+h)^2}}+\sum_{n=1}^{\infty} Q^n[\frac{2nd-z-h}{\sqrt{r^2+(2nd-z-h)^2}} \tag{30}$$

$$-\frac{2nd+z+h}{\sqrt{r^2+(2nd+z+h)^2}}+\frac{2nd-z+h}{\sqrt{r^2+(2nd-z+h)^2}}-\frac{2nd+z-h}{\sqrt{r^2+(2nd+z-h)^2}}]\}$$

$$(h < z \le d).$$

Next, region 1 is examined for the case $0 \le z < h$. Consistent application of Ampere's Law for this case requires that the contribution of the line current be included, and then

$$2\pi r H_\theta = I + 2\pi \int_0^r du\, u J_z \tag{31}$$

and this time substitution from Equation (23) with careful attention to the relative values of z and h, yields

$$H_{1\theta}=\frac{I}{4\pi r}\{2-\frac{z-h}{\sqrt{r^2+(z-h)^2}}-\frac{z+h}{\sqrt{r^2+(z+h)^2}}+\sum_{n=1}^{\infty}Q^n[\frac{2nd-z-h}{\sqrt{r^2+(2nd-z-h)^2}} \tag{32}$$

$$-\frac{2nd+z+h}{\sqrt{r^2+(2nd+z+h)^2}}+\frac{2nd-z+h}{\sqrt{r^2+(2nd-z+h)^2}}-\frac{2nd+z-h}{\sqrt{r^2+(2nd+z-h)^2}}]\}$$

$$(0 \le z < h),$$

which is identical in form to Equation (30), and the magnetic field is continuous at the electrode $(z = h)$ plane, as it must be to be physical.

Now, to isolate the magnetic field due to the electrode distributed currents alone, the Biot-Savart magnetic field of the wire alone is constructed and it is subtracted from the expressions in Equations (29), (30), and (32). Then

$$H_\theta^{bs}=\frac{I}{4\pi r}\left[1-\frac{(z-h)}{\sqrt{r^2+(z-h)^2}}\right] \tag{33}$$

and the electrode magnetic field alone, everywhere in region 1, is given by

$$H_{1\theta}^e=\frac{I}{4\pi r}\{1-\frac{z+h}{\sqrt{r^2+(z+h)^2}}+\sum_{n=1}^{\infty}Q^n[\frac{2nd-z-h}{\sqrt{r^2+(2nd-z-h)^2}} \tag{34}$$

$$-\frac{2nd+z+h}{\sqrt{r^2+(2nd+z+h)^2}}+\frac{2nd-z+h}{\sqrt{r^2+(2nd-z+h)^2}}-\frac{2nd+z-h}{\sqrt{r^2+(2nd+z-h)^2}}]\}$$

$$(0 \le z \le d),$$

and in region 2, the field is

$$H_{2\theta}^e=\frac{I}{4\pi r}\left\{1+\frac{z-h}{\sqrt{r^2+(z-h)^2}}-(1-Q)\sum_{n=0}^{\infty}Q^n\left[\frac{2nd+z-h}{\sqrt{r^2+2nd+z-h^2}}+\frac{2nd+z+h}{\sqrt{r^2+2nd+z+h^2}}\right]\right\}. \tag{35}$$

Then the cartesian components in either region are given by

$$H_x^e=-\frac{y}{r}H_\theta^e \quad \text{and} \quad H_y^e=\frac{x}{r}H_\theta^e. \tag{36}$$

NON-CONDUCTING BOTTOM (Q=1)

Region 1

In the limit of a non-conducting bottom, $Q = 1$, and the series solutions for the fields diverge. To deal with the fields in region 1, the integral expressions defining them will be revisited. The current density is determined from Equations (9) and (17) and has the form

$$J_{1x(y)} = \frac{Ix(y)}{4\pi r}\int_0^\infty d\lambda\lambda J_1(\lambda r)\{e^{-\lambda|z-h|} + e^{-\lambda(z+h)} \tag{37}$$

$$+\frac{e^{-2\lambda d}}{1-e^{-2\lambda d}}[e^{\lambda(z+h)} + e^{-\lambda(z+h)} + e^{\lambda(z-h)} + e^{-\lambda(z-h)}]\}$$

and

$$J_{1z} = \frac{I}{4\pi}\int_0^\infty d\lambda\lambda J_0(\lambda r)\{sgn(z-h)e^{-\lambda|z-h|} + e^{-\lambda(z+h)} \tag{38}$$

$$+\frac{e^{-2\lambda d}}{1-e^{-2\lambda d}}[-e^{\lambda(z+h)} + e^{-\lambda(z+h)} - e^{\lambda(z-h)} + e^{-\lambda(z-h)}]\}.$$

The case $z > h$ is explicitly selected. The end result is the same for any case. The expression for the electrode magnetic field is then obtained by combining Equations (26) through (28), (33), and (38). The result is

$$H^e_{1\theta} = \frac{I}{4\pi r}(-1 + \frac{z-h}{\sqrt{r^2+(z-h)^2}} + r\int_0^\infty d\lambda J_1(\lambda r)\{e^{-\lambda(z-h)} + e^{-\lambda(z+h)} \tag{39}$$

$$+\frac{e^{-2\lambda d}}{1-e^{-2\lambda d}}[-e^{\lambda(z+h)} + e^{-\lambda(z+h)} - e^{\lambda(z-h)} + e^{-\lambda(z-h)}]\}).$$

In each of Equations (37) through (39) a common denominator is used and terms are combined into hyperbolic functions. Then, the fields have the forms

$$J_{1x(y)} = \frac{Ix(y)}{4\pi r}\int_0^\infty d\lambda\lambda J_1(\lambda r)\left\{\frac{\cosh[\lambda(d-z+h)] + \cosh[\lambda(d-z-h)]}{\sinh(\lambda d)}\right\} \tag{40}$$

$$J_{1z} = \frac{I}{4\pi}\int_0^\infty d\lambda\lambda J_0(\lambda r)\left\{\frac{\sinh[\lambda(d-z+h)] + \sinh[\lambda(d-z-h)]}{\sinh(\lambda d)}\right\} \tag{41}$$

and

$$H^e_{1\theta} = \frac{I}{4\pi r}(-1 + \frac{z-h}{\sqrt{r^2+(z-h)^2}} \tag{42}$$

$$+r\int_0^\infty d\lambda J_1(\lambda r)\left\{\frac{\sinh[\lambda(d-z+h)] + \sinh[\lambda(d-z-h)]}{\sinh(\lambda d)}\right\}).$$

There are three integral types; they are

$$\iota_1 = \int_0^\infty d\lambda \lambda J_1(\lambda r) \frac{\cosh(\lambda a)}{\sinh(\lambda d)} \tag{43}$$

$$\iota_2 = \int_0^\infty d\lambda \lambda J_0(\lambda r) \frac{\sinh(\lambda a)}{\sinh(\lambda d)} \tag{44}$$

and

$$\iota_3 = \int_0^\infty d\lambda J_1(\lambda r) \frac{\sinh(\lambda a)}{\sinh(\lambda d)}. \tag{45}$$

Contour Integration-Residue Theorem. If the integrands of ι_1, ι_2, and ι_3 are analytically continued into the complex plane $\lambda \to w = u + iv$, the denominator $\sinh(wd)$ will have zeros for $wd = in\pi$, where $n = 0, \pm 1, \pm 2, \cdots$. This suggests that the required integrals be related to integrals over a closed contour containing these zeros, and the Cauchy residue theorem be exploited. An appropriate contour is shown in Figure 3. The contour is closed in the upper half plane, and the zeros involved are those for $n > 0$.

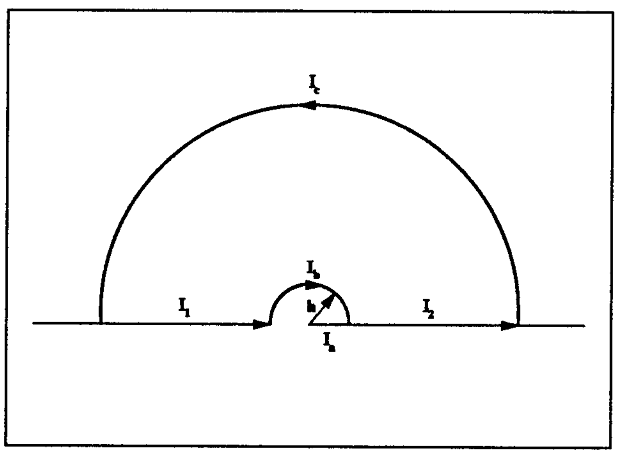

FIGURE 3. INTEGRATION CONTOUR IN w PLANE

The integrals of interest are taken over the interval I_2 in Figure 3, in the limit that I_a goes to 0, and I_2 becomes infinite. This integral will be related to the closed contour integral over the successive intervals I_1, I_b, I_2, and I_c. To this end, the integral over I_2 will be expressed in terms of an integral over both I_1 and I_2. To accomplish this, bessel functions J_n will be expressed in terms of hankel functions. This relationship is analogous to the representation of the cosine function by means of complex exponentials, which is a trick used in fourier transform theory to extend integrals from the positive real axis to the entire real axis. The hankel functions are defined by

$$H_n^{(1)}(z) = J_n(z) + iY_n(z) \tag{46}$$

$$H_n^{(2)}(z) = J_n(z) - iY_n(z)$$

where Y_n is the bessel function irregular at the origin. The bessel function J_n, which is regular at the origin, now can be expressed as

$$J_n(z) = \frac{1}{2}[H_n^{(1)}(z) + H_n^{(2)}(z)]. \tag{47}$$

Next, it is noted that the hankel functions have the symmetry properties

$$H_0^{(1)}(-z) = -H_0^{(2)}(z) \tag{48}$$

$$H_1^{(1)}(-z) = H_1^{(2)}(z).$$

Inserting Equation (47) in Equation (43), for example, and using the symmetry properties of all the factors in the integrand, gives

$$\int_{I_2} d\lambda\lambda J_1(\lambda r)\frac{\cosh(\lambda a)}{\sinh(\lambda d)} \tag{49}$$

$$= \frac{1}{2}\int_{I_2} d\lambda\lambda H_1^{(1)}(\lambda r)\frac{\cosh(\lambda a)}{\sinh(\lambda d)} + \frac{1}{2}\int_{I_2} d\lambda\lambda H_1^{(2)}(\lambda r)\frac{\cosh(\lambda a)}{\sinh(\lambda d)}$$

$$= \frac{1}{2}\int_{I_2} d\lambda\lambda H_1^{(1)}(\lambda r)\frac{\cosh(\lambda a)}{\sinh(\lambda d)} + \frac{1}{2}\int_{-I_2} d(-\lambda)(-\lambda)H_1^{(2)}(-\lambda r)\frac{\cosh(-\lambda a)}{\sinh(-\lambda d)}$$

$$= \frac{1}{2}\int_{I_1\&I_2} d\lambda\lambda H_1^{(1)}(\lambda r)\frac{\cosh(\lambda a)}{\sinh(\lambda d)}$$

where the relation has been used for the intervals $-(-I_2) = I_1$. Thus, the integral over I_2 is replaced by an integral over I_1 and I_2, with J_1 replaced by $H_1^{(1)}/2$. A similar operation can be done for the integrals in Equations (44) and (45).

Now, using a shorthand notation, relations between the integrals over the various contour segments can be written, where it is understood that the equations hold in the limit that the inner semicircle shrinks to zero, and the outer semicircle recedes to infinity. Then

$$\iota = \int_{I_1\&I_2} + \int_{I_a} \tag{50}$$

and

$$\oint = \int_{I_1 \& I_2} + \int_{I_b} + \int_{I_c} \tag{51}$$

where $\oint$ is the integral around the closed contour. Thus

$$\imath = \oint - \int_{I_b} - \int_{I_c} + \int_{I_a} . \tag{52}$$

The following generic results hold for the three integrals of interest.

$$\oint \rightarrow 2\pi i \sum_{n=1}^{\infty} S_n \tag{53}$$

$$\int_{I_a} \rightarrow 0, \quad \text{(all cases)} \tag{54}$$

$$\int_{I_c} \rightarrow 0, \quad \text{(all cases)} \tag{55}$$

$$\int_{I_b} \rightarrow \text{(simple limit)} \tag{56}$$

Here, the S_n are the residues, defined by

$$\oint dw f(w) = \oint dw \frac{f(w)(w-w_0)}{w-w_0} = \oint dw \frac{g(w)}{w-w_0}, \tag{57}$$

$$S_n = \lim_{w \rightarrow w_0} g(w) \,|_{w_0 = in\pi/d} \, .$$

To establish the limiting values of the various integrals, the limiting forms of the functions involved are examined;

$$J_0(u) \rightarrow 1, \quad J_1(u) \rightarrow u, \quad u \rightarrow 0 \tag{58}$$

$$\cosh(w) \rightarrow 1, \quad \sinh(w) \rightarrow w, \quad |w| \rightarrow 0 \tag{59}$$

$$H_0^{(1)}(w) \rightarrow \frac{2i}{\pi}[\ln(w/2)+\gamma], \quad H_1^{(1)}(w) \rightarrow -\frac{2i}{\pi w}, \quad |w| \rightarrow 0 \tag{60}$$

$$(\gamma = 0.5772156649 \cdots \text{Euler's constant})$$

and

$$H_0^{(1)}(w) \to \frac{(1-i)e^{iw}}{\sqrt{\pi w}}, \quad H_1^{(1)}(w) \to -\frac{(1+i)e^{iw}}{\sqrt{\pi w}}, \quad |w| \to \infty. \tag{61}$$

Applying Equations (58) and (59) to the integrands of ι_1, ι_2 and ι_3 shows that the integrands approach 0 as λ approaches 0, establishing Equation (54). For the integrals on contour I_c, $w = Re^{i\phi}$, and the hankel function factor in the integrands has the behavior

$$\frac{e^{-rR\sin\phi}}{\sqrt{rR}} \to 0, \quad R \to \infty. \tag{62}$$

The other factors are all proportional to the limiting form

$$e^{(a-d)R|\cos\phi|}, \quad R \to \infty. \tag{63}$$

For $\phi = \pi/2$, the associated factors are purely oscillatory, and are dominated by the decaying hankel function factor. For other angles

$$a-d = d-z+h-d = -(z-h) < 0, \quad \text{or} \quad a-d = d-z-h-d = -(z+h) < 0 \tag{64}$$

and the factor vanishes as $R \to \infty$. This establishes Equation (55).

To determine the limiting forms for the integrals over the contour I_b, let $w = he^{i\phi}$, and explicitly list the integrals. They are

$$\frac{1}{2}\int_{\pi}^{0} d\phi\, ih^2 e^{2i\phi} \frac{-2i}{\pi h r e^{i\phi}} \frac{1}{h d e^{i\phi}} = \frac{1}{\pi r d}\int_{\pi}^{0} d\phi \to -\frac{1}{rd}, \quad h \to 0 \tag{65}$$

$$\frac{1}{2}\int_{\pi}^{0} d\phi\, ih^2 e^{2i\phi} \frac{2i}{\pi}\left[\ln\left(\frac{h}{2}e^{i\phi}\right)+\gamma\right]\frac{hae^{i\phi}}{hde^{i\phi}} \to 0, \quad h \to 0 \tag{66}$$

and

$$\frac{1}{2}\int_{\pi}^{0} d\phi\, ihe^{i\phi} \frac{-2i}{\pi h r e^{i\phi}} \frac{hae^{i\phi}}{hde^{i\phi}} = \frac{a}{\pi r d}\int_{\pi}^{0} d\phi \to -\frac{a}{rd}, \quad h \to 0. \tag{67}$$

The residues are constructed using a simple limit process, as indicated in Equation (57). Some useful expressions for the evaluations are

$$\sinh(dw) = \cosh(dw_n)d(w-w_n) + \cdots, \quad w \to w_n \tag{68}$$

where dw_n is a zero of $\sinh(dw)$,

$$\cosh(iu) = \cos(u) \tag{69}$$

$$\sinh(iu) = i\sin(u)$$

and

$$H_0^{(1)}(iu) = -\frac{2i}{\pi}K_0(u) \tag{70}$$

$$H_1^{(1)}(iu) = -\frac{2}{\pi}K_1(u)$$

where the K_n are the modified bessel functions regular at infinity. Using these results, the residues can be written as

$$\frac{1}{2}wH_1^{(1)}(rw)\frac{\cosh(aw)}{\sinh(dw)}(w - in\pi/d) \rightarrow \frac{in\pi}{2d}H_1^{(1)}(in\pi r/d)\frac{\cosh(in\pi a/d)}{(-1)^n d} \tag{71}$$

$$= -\frac{i}{d^2}n(-1)^n K_1(n\pi r/d)\cos(n\pi a/d)$$

$$\frac{1}{2}wH_0^{(1)}(rw)\frac{\sinh(aw)}{\sinh(dw)}(w - in\pi/d) \rightarrow \frac{in\pi}{2d}H_0^{(1)}(in\pi r/d)\frac{\sinh(in\pi a/d)}{(-1)^n d} \tag{72}$$

$$= \frac{i}{d^2}n(-1)^n K_0(n\pi r/d)\sin(n\pi a/d)$$

and

$$\frac{1}{2}H_1^{(1)}(rw)\frac{\sinh(aw)}{\sinh(dw)}(w - in\pi/d) \rightarrow \frac{1}{2}H_1^{(1)}(in\pi r/d)\frac{\sinh(in\pi a/d)}{(-1)^n d} \tag{73}$$

$$= -\frac{i}{\pi d}(-1)^n K_1(n\pi r/d)\sin(n\pi a/d).$$

Now the explicit forms for the fields can be constructed. In doing so, the arguments of the trigonometric functions are expanded and integral multiples of π are eliminated. Now

$$\imath = \oint - \int_{l_b} \tag{74}$$

and Equations (40) through (42), Equation (53), Equations (65) through (67), and Equations (71) through (73) are combined. The results are

$$J_{1x(y)} = \frac{Ix(y)}{2\pi d r^2}\left(1 + \frac{\pi r}{d}\sum_{n=1}^{\infty} nK_1(n\pi r/d)\left[\cos\{n\pi(z-h)/d\} + \cos\{n\pi(z+h)/d\}\right]\right) \tag{75}$$

$$J_{1z}=\frac{I}{2d^2}\sum_{n=1}^{\infty} nK_0(n\pi r/d)\,[\sin\{n\pi(z-h)/d\}+\sin\{n\pi(z+h)/d\}] \tag{76}$$

and, subtracting the Biot-Savart field (Equation (33)),

$$H^e_{1\theta}=\frac{I}{4\pi r}(1+\frac{z-h}{\sqrt{r^2+(z-h)^2}}-\frac{2z}{d} \tag{77}$$

$$+\frac{\pi r}{d}\sum_{n=1}^{\infty} K_1(n\pi r/d)\,[\sin\{n\pi(z-h)/d\}+\sin\{n\pi(z+h)/d\}]).$$

<u>Region 2</u>

Inspection of Equations (24), (25), and (35) shows that the fields reduce to the simple forms

$$J_{2x(y)}=0 \tag{78}$$

$$J_{2z}=0 \tag{79}$$

and

$$H^e_{2\theta}=\frac{I}{4\pi r}\left[1+\frac{z-h}{\sqrt{r^2+(z-h)^2}}\right]. \tag{80}$$

PERFECTLY CONDUCTING BOTTOM (Q=-1, REGION 1 ONLY)

<u>Region 1</u>

In this case, when the various terms in region 1 are combined to give hyperbolic functions, the resulting integrals are

$$J_{1x(y)}=\frac{Ix(y)}{4\pi r}\int_0^{\infty} d\lambda\lambda J_1(\lambda r)\left\{\frac{\sinh[\lambda(d-z+h)]+\sinh[\lambda(d-z-h)]}{\cosh(\lambda d)}\right\} \tag{81}$$

$$J_{1z}=\frac{I}{4\pi}\int_0^{\infty} d\lambda\lambda J_0(\lambda r)\left\{\frac{\cosh[\lambda(d-z+h)]+\cosh[\lambda(d-z-h)]}{\cosh(\lambda d)}\right\} \tag{82}$$

and

$$H^e_{1\theta}=\frac{I}{4\pi}\int_0^{\infty} d\lambda J_1(\lambda r)\left\{\frac{\cosh[\lambda(d-z+h)]+\cosh[\lambda(d-z-h)]}{\cosh(\lambda d)}\right\}. \tag{83}$$

The three types of integral now are

$$\iota_1 = \int_0^\infty d\lambda \lambda J_1(\lambda r) \frac{\sinh(\lambda a)}{\cosh(\lambda d)} \tag{84}$$

$$\iota_2 = \int_0^\infty d\lambda \lambda J_0(\lambda r) \frac{\cosh(\lambda a)}{\cosh(\lambda d)} \tag{85}$$

and

$$\iota_3 = \int_0^\infty d\lambda J_1(\lambda r) \frac{\cosh(\lambda a)}{\cosh(\lambda d)}. \tag{86}$$

Again the construct of Equation (49) can be used to introduce the hankel function, and analytic continuation and the residue theorem can be used, where now the singularities occur for

$$z = i(n + 1/2)\pi/d, \quad n = 0, \pm 1, \pm 2, \ldots \tag{87}$$

Again,

$$\iota = \oint - \int_{I_b} - \int_{I_c} + \int_{I_a} \tag{88}$$

and, again

$$I_a \to 0 \quad \text{and} \quad I_c \to 0. \tag{89}$$

Now, for I_b

$$\frac{1}{2}\int_\pi^0 d\phi\, i h^2 e^{2i\phi} \frac{-2i}{\pi h r e^{i\phi}} \frac{a h e^{i\phi}}{1} \to 0 \tag{90}$$

$$\frac{1}{2}\int_\pi^0 d\phi\, i h^2 e^{2i\phi} \left[\frac{2i}{\pi} \ln\left(\frac{h r e^{i\phi}}{2} \right) + \gamma \right] \frac{1}{1} \to 0 \tag{91}$$

$$\frac{1}{2}\int_\pi^0 d\phi\, i h e^{i\phi} \frac{-2i}{\pi h r e^{i\phi}} \frac{1}{1} \to -\frac{1}{r} \tag{92}$$

and for the residues S_n

$$\frac{1}{2} w H_1^{(1)}(rw) \frac{\sinh(aw)}{\cosh(dw)} [w - i(n+1/2)\pi/d] \tag{93}$$

$$\rightarrow \frac{1}{2}[i(n+1/2)\pi/d] H_1^{(1)}[i(n+1/2)\pi r/d] \sinh[i(n+1/2)\pi a/d] \frac{1}{i(-1)^n d}$$

$$= \frac{i(n+1/2)(-1)^{n+1}}{d^2} K_1[(n+1/2)\pi r/d] \sin[(n+1/2)\pi a/d]$$

$$\frac{1}{2} w H_0^{(1)}(rw) \frac{\cosh(aw)}{\cosh(dw)} [w - i(n+1/2)\pi/d] \tag{94}$$

$$\rightarrow \frac{1}{2}[(n+1/2)\pi/d] H_0^{(1)}[i(n+1/2)\pi r/d] \cosh[i(n+1/2)\pi a/d] \frac{1}{(-1)^n d}$$

$$= \frac{i(n+1/2)(-1)^{n+1}}{d^2} K_0[(n+1/2)\pi r/d] \cos[(n+1/2)\pi a/d]$$

$$\frac{1}{2} H_1^{(1)}(rw) \frac{\cosh(aw)}{\cosh(dw)} [w - i(n+1/2)\pi/d] \tag{95}$$

$$\rightarrow \frac{1}{2} H_1^{(1)}[i(n+1/2)\pi r/d] \cosh[i(n+1/2)\pi a/d] \frac{1}{i(-1)^n d}$$

$$= \frac{i(-1)^n}{\pi d} K_1[(n+1/2)\pi r/d] \cos[(n+1/2)\pi a/d].$$

Then, using

$$\imath = \oint - I_b = 2\pi i \sum_{n=1}^{\infty} S_n - I_b \tag{96}$$

gives

$$J_{1x(y)} = \frac{Ix(y)}{2rd^2} \sum_{n=0}^{\infty} (n+1/2) K_1[(n+1/2)\pi r/d] \tag{97}$$

$$\{\cos[(n+1/2)\pi(z-h)/d] + \cos[(n+1/2)\pi(z+h)/d]\}$$

$$J_{1z} = \frac{I}{2d^2} \sum_{n=0}^{\infty} (n+1/2) K_0[(n+1/2)\pi r/d] \tag{98}$$

$$\{\sin[(n+1/2)\pi(z-h)/d] + \sin[(n+1/2)\pi(z+h)/d]\}$$

and, again subtracting the Biot-Savart field (Equation (33)),

$$H_{1\theta} = \frac{I}{4\pi r}(1 + \frac{z-h}{\sqrt{r^2 + (z-h)^2}} - \frac{2r}{d}\sum_{n=0}^{\infty} K_1[(n+1/2)\pi r/d] \tag{99}$$

$$\{\sin[(n+1/2)\pi(z-h)/d] + \sin[(n+1/2)\pi(z+h)/d]\}).$$

Region 2

In region 2, the integral forms for the fields are

$$J_{2x(y)} = \frac{x(y)I}{2\pi r}\int_0^{\infty} d\lambda\lambda J_1(\lambda r)\left[\frac{e^{-\lambda(z+h)} + e^{-\lambda(z-h)}}{1+e^{-2\lambda d}}\right] \tag{100}$$

$$J_{2z} = \frac{I}{2\pi}\int_0^{\infty} d\lambda\lambda J_0(\lambda r)\left[\frac{e^{-\lambda(z+h)} + e^{-\lambda(z-h)}}{1+e^{-2\lambda d}}\right] \tag{101}$$

and

$$H_{2\theta}^{e} = \frac{I}{4\pi r}\{-1 + \frac{z-h}{\sqrt{r^2+(z-h)^2}} \tag{102}$$

$$+2r\int_0^{\infty} d\lambda J_1(\lambda r)\left[\frac{e^{-\lambda(z+h)} + e^{-\lambda(z-h)}}{1+e^{-2\lambda d}}\right]\}.$$

In these integrals, the denominator can be converted to a hyperbolic cosine, but the numerators will be linear combinations of hyperbolic sine and cosine functions. Some of the terms can be rewritten using a construct similar to Equation (49), and can be treated with contour integration techniques. However, the remaining terms do not have the appropriate symmetry to accomplish this. These remaining terms have symmetry such that the integral can be extended over the real axis while retaining the bessel function form, and there is no singularity at the origin as there is with the hankel function. However, when the integrands of these terms are analytically continued into the complex plane, the bessel functions diverge in either half plane, and the outer contour cannot be closed. Thus, there is no way to explicitly evaluate these integrals. As this particular case is more of a curiosity without practical significance, it will not be pursued further.

DISTRIBUTED CURRENT MAGNETIC FIELD GRADIENT

The magnetic field gradients due to the electrode distributed currents can be expressed in terms of the r and z derivatives of the magnetic field expressions already obtained in Equations (34), (35), (77), (80), and (99). First

$$H_x^e = -H_\theta^e \sin\theta = -\frac{y}{r}H_\theta^e \tag{103}$$

and

$$H_y^e = H_\theta^e \cos\theta = \frac{x}{r} H_\theta^e. \tag{104}$$

Then, for the diagonal gradients

$$\frac{\partial H_x^e}{\partial x} = \frac{xy}{r^3} - \frac{y}{r}\frac{\partial H_\theta^e}{\partial x} = \frac{xy}{r^2}\left(\frac{H_\theta^e}{r} - \frac{\partial H_\theta^e}{\partial r}\right) \tag{105}$$

and

$$\frac{\partial H_y^e}{\partial y} = -\frac{\partial H_x^e}{\partial x}, \tag{106}$$

the latter following from $\nabla \cdot \mathbf{H}^e = 0$ and $H_z^e = 0$ ($\nabla \cdot \mathbf{H} = 0$ and below, it is shown that $\nabla \cdot \mathbf{H}^{BS} = 0$).

For the off-diagonal gradients, the non-zero terms are

$$\frac{\partial H_x^e}{\partial z} = -\frac{y}{r}\frac{\partial H_\theta^e}{\partial z} \tag{107}$$

$$\frac{\partial H_y^e}{\partial z} = \frac{x}{r}\frac{\partial H_\theta^e}{\partial z} \tag{108}$$

$$\frac{\partial H_x^e}{\partial y} = -\left[\frac{x^2}{r^3}H_\theta^e + \frac{y^2}{r^2}\frac{\partial H_\theta^e}{\partial r}\right] \tag{109}$$

and

$$\frac{\partial H_y^e}{\partial x} = \left[\frac{y^2}{r^3}H_\theta^e + \frac{x^2}{r^2}\frac{\partial H_\theta^e}{\partial r}\right]. \tag{110}$$

CONDUCTING BOTTOM

<u>Region 1</u>

From Equation (34)

$$\frac{\partial H_{1\theta}^e}{\partial r} = -\frac{H_{1\theta}^e}{r} + \frac{I}{4\pi}\Big[\frac{z+h}{\sqrt{(r^2+(z+h)^2)^3}} + \sum_{n=1}^{\infty} Q^n\Big\{-\frac{2nd-z-h}{\sqrt{(r^2+(2nd-z-h)^2)^3}} \tag{111}$$
$$+\frac{2nd+z+h}{\sqrt{(r^2+(2nd+z+h)^2)^3}} - \frac{2nd-z+h}{\sqrt{(r^2+(2nd-z+h)^2)^3}} + \frac{2nd+z-h}{\sqrt{(r^2+(2nd+z-h)^2)^3}}\Big\}\Big].$$

and

$$\frac{\partial H^e_{1\theta}}{\partial z}=\frac{I}{4\pi r}[\frac{(z+h)^2}{\sqrt{(r^2+(z+h)^2)^3}}-\frac{1}{\sqrt{r^2+(z+h)^2}}+\sum_{n=1}^{\infty}Q^n\{\frac{(2nd-z-h)^2}{\sqrt{(r^2+(2nd-z-h)^2)^3}} \tag{112}$$

$$+\frac{(2nd+z+h)^2}{\sqrt{(r^2+(2nd+z+h)^2)^3}}+\frac{(2nd-z+h)^2}{\sqrt{(r^2+(2nd-z+h)^2)^3}}+\frac{(2nd+z-h)^2}{\sqrt{(r^2+(2nd+z-h)^2)^3}}$$

$$-\frac{1}{\sqrt{r^2+(2nd-z-h)^2}}-\frac{1}{\sqrt{r^2+(2nd+z+h)^2}}-\frac{1}{\sqrt{r^2+(2nd-z+h)^2}}-\frac{1}{\sqrt{r^2+(2nd+z-h)^2}}\}]$$

<u>Region 2</u>

From Equation (35)

$$\frac{\partial H^e_{2\theta}}{\partial r}=-\frac{H^e_{2\theta}}{r}+\frac{I}{4\pi}\{-\frac{z-h}{\sqrt{(r^2+(z-h)^2)^3}} \tag{113}$$

$$+(1-Q)\sum_{n=0}^{\infty}Q^n\left[\frac{2nd+z-h}{\sqrt{(r^2+2nd+z-h^2)^3}}+\frac{2nd+z+h}{\sqrt{(r^2+2nd+z+h^2)^3}}\right]\}$$

and

$$\frac{\partial H^e_{2\theta}}{\partial z}=\frac{I}{4\pi r}\{-\frac{(z-h)^2}{\sqrt{(r^2+(z-h)^2)^3}} \tag{114}$$

$$+(1-Q)\sum_{n=0}^{\infty}Q^n\left[\frac{(2nd+z-h)^2}{\sqrt{(r^2+2nd+z-h^2)^3}}+\frac{(2nd+z+h)^2}{\sqrt{(r^2+2nd+z+h^2)^3}}\right]\}.$$

NON-CONDUCTING BOTTOM (Q=1)

<u>Region 1</u>

From Equation (77)

$$\frac{\partial H^e_{1\theta}}{\partial r}=\frac{I}{4\pi}(-\frac{1}{r^2}\left[1+\frac{z-h}{\sqrt{r^2+(z-h)^2}}-\frac{2z}{d}\right]-\frac{z-h}{\sqrt{(r^2+(z-h)^2)^3}} \tag{115}$$

$$+\frac{\pi^2}{d^2}\sum_{n=1}^{\infty}nK_0(n\pi r/d)[\sin\{n\pi(z-h)/d\}+\sin\{n\pi(z+h)/d\}])$$

and

$$\frac{\partial H_{1\theta}^{e}}{\partial z}=\frac{I}{4\pi r}\left(\frac{1}{\sqrt{r^2+(z-h)^2}}-\frac{(z-h)^2}{\sqrt{(r^2+(z-h)^2)^3}}-\frac{2}{d}\right. \tag{116}$$

$$\left.+r\frac{\pi^2}{d^2}\sum_{n=1}^{\infty}nK_1(n\pi r/d)[\cos\{n\pi(z-h)/d\}+\cos\{n\pi(z+h)/d\}]\right).$$

<u>Region 2</u>

From Equation (80)

$$\frac{\partial H_{2\theta}^{e}}{\partial r}=-\frac{H_{2\theta}^{e}}{r}-\frac{I}{4\pi}\left[\frac{z-h}{\sqrt{(r^2+(z-h)^2)^3}}\right]. \tag{117}$$

and

$$\frac{\partial H_{2\theta}^{e}}{\partial z}=-\frac{I}{4\pi r}\left[\frac{(z-h)^2}{\sqrt{(r^2+(z-h)^2)^3}}\right]. \tag{118}$$

PERFECTLY CONDUCTING BOTTOM (Q=-1, REGION 1 ONLY)

From Equation (99)

$$\frac{\partial H_{1\theta}^{e}}{\partial r}=\frac{I}{4\pi}\left(-\frac{z-h}{r^2\sqrt{r^2+(z-h)^2}}-\frac{z-h}{\sqrt{(r^2+(z-h)^2)^3}}-\frac{2\pi}{d^2}\sum_{n=0}^{\infty}(n+1/2)K_1[(n+1/2)\pi r/d]\right. \tag{119}$$

$$\left.\{\sin[(n+1/2)\pi(z-h)/d]+\sin[(n+1/2)\pi(z+h)/d]\}\right)$$

and

$$\frac{\partial H_{1\theta}^{e}}{\partial z}=\frac{I}{4\pi r}\left(-\frac{(z-h)^2}{\sqrt{(r^2+(z-h)^2)^3}}+\frac{1}{\sqrt{r^2+(z-h)^2}}-\frac{2\pi r}{d^2}\sum_{n=0}^{\infty}(n+1/2)K_1[(n+1/2)\pi r/d]\right. \tag{120}$$

$$\left.\{\cos[(n+1/2)\pi(z-h)/d]+\cos[(n+1/2)\pi(z+h)/d]\}\right).$$

MAGNETIC FIELD/FIELD GRADIENT GENERATED BY A CABLE TERMINATED IN REGION 1: CABLE-ONLY CONTRIBUTION

The magnetic field/field gradient of a cable carrying a current I, with each end shorted to the medium in region 1, can be constructed as the superposition of the magnetic field/field gradient of an electrode at each cable end point and the Biot-Savart magnetic field/field gradient of the cable current. The configuration is shown in Figure 4.

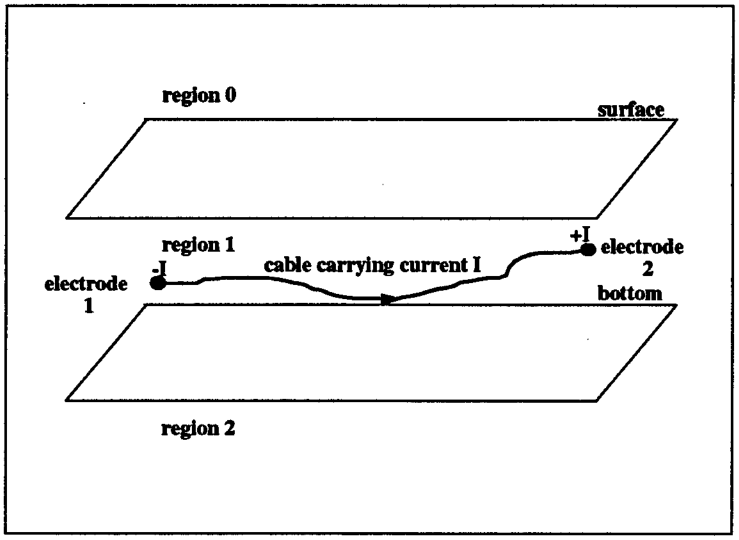

FIGURE 4. CURRENT-CARRYING CABLE/ELECTRODE CONFIGURATION

The electrode contributions to the magnetic field are constructed by means of Equations (34) through (36) with appropriate assignments of geometry and with current signs as indicated in Figure 4. The electrode contributions to the magnetic field gradient tensor are detailed in Equations (105) through (120). The contribution of the cable is obtained by means of a line integral along the cable. In practice, the line integral is approximated as a sum of line integrals over short linear segments. A general representation is now given of the magnetic field vector and gradient tensor for such a segment.

BIOT-SAVART FIELD AND GRADIENT OF A STRAIGHT CABLE SEGMENT

The geometry for the construction is shown in Figure 5. Vector quantities there are indicated with superposed arrows, but in the text they are indicated with boldface type. The various vectors involved are

$\mathbf{R}_1, \mathbf{R}_2$ locate cable segment end points ($1 \rightarrow 2$ positive current flow)

$\mathbf{R}$ locates the field point

$\mathbf{R}_2 - \mathbf{R}_1$ is along the cable segment

$$\hat{\mathbf{l}} = \frac{\mathbf{R}_2 - \mathbf{R}_1}{|\mathbf{R}_2 - \mathbf{R}_1|}, \quad \hat{\mathbf{u}}_1 = \frac{\mathbf{R}_1 - \mathbf{R}}{|\mathbf{R}_1 - \mathbf{R}|}, \quad \text{and} \quad \hat{\mathbf{u}}_2 = \frac{\mathbf{R}_2 - \mathbf{R}}{|\mathbf{R}_2 - \mathbf{R}|} \quad \text{are unit vectors.}$$

With these definitions, the general expression for the magnetic field of the cable segment can be given. This expression is the result of analytically performing the line integral

$$\mathbf{H}=\frac{I}{4\pi}\int_{\mathbf{R}_1}^{\mathbf{R}_2}\frac{d\mathbf{l}'\times(\mathbf{R}-\mathbf{R}')}{|\mathbf{R}-\mathbf{R}'|^3}=\frac{I}{4\pi}\hat{\mathbf{l}}\times(\mathbf{R}-\mathbf{R}_1)I_1 \tag{121}$$

$$=\frac{I}{4\pi}\hat{\mathbf{l}}\times(\mathbf{R}-\mathbf{R}_1)\int_0^{|\mathbf{R}_1-\mathbf{R}_2|}\frac{du}{\left(\sqrt{u^2-2\hat{\mathbf{l}}\cdot(\mathbf{R}-\mathbf{R}_1)u+|\mathbf{R}-\mathbf{R}_1|^2}\right)^3}$$

over the straight segment, and using some results from vector geometry. The result is

$$I_1=\frac{1}{|\mathbf{R}-\mathbf{R}_1|^2}\left[\frac{\hat{\mathbf{l}}\cdot(\hat{\mathbf{u}}_2-\hat{\mathbf{u}}_1)}{1-(\hat{\mathbf{l}}\cdot\hat{\mathbf{u}}_1)^2}\right] \tag{122}$$

and

$$\mathbf{H}=\frac{I}{4\pi|\mathbf{R}_1-\mathbf{R}|}\hat{\mathbf{u}}_1\times\hat{\mathbf{l}}\left[\frac{\hat{\mathbf{l}}\cdot(\hat{\mathbf{u}}_2-\hat{\mathbf{u}}_1)}{1-(\hat{\mathbf{u}}_1\cdot\hat{\mathbf{l}})^2}\right]. \tag{123}$$

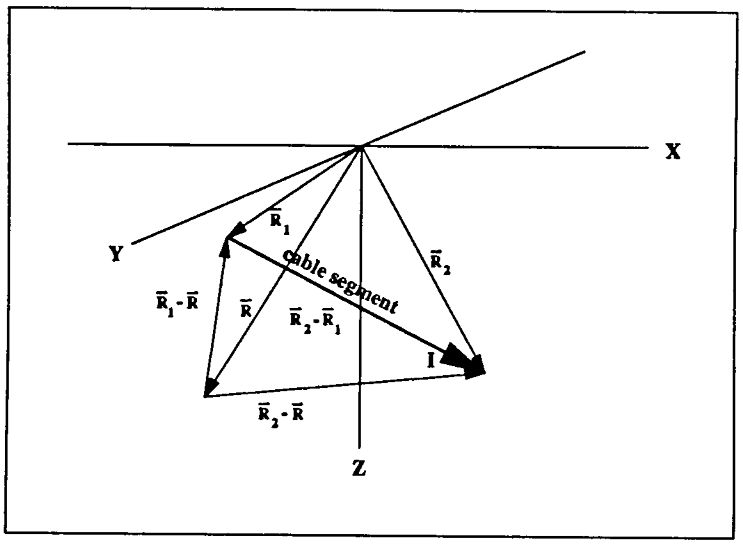

FIGURE 5. CABLE SEGMENT GEOMETRY

The field gradient tensor is best constructed by writing out Equation (121) in component form and taking the appropriate derivatives. Then

$$H_i=\frac{I}{4\pi}\varepsilon_{imn}\hat{l}_m(R_n-R_{1n})\int_0^{|\mathbf{R}_1-\mathbf{R}_2|}\frac{du}{\left(\sqrt{u^2-2\hat{\mathbf{l}}\cdot(\mathbf{R}-\mathbf{R}_1)u+|\mathbf{R}-\mathbf{R}_1|^2}\right)^3} \tag{124}$$

where the Levi-Civita tensor ε_{imn} has the properties

$$\varepsilon_{imn} = 1 \quad \text{i,m,n an even permutation of 1,2,3} \tag{125}$$

$$\varepsilon_{imn} = -1 \quad \text{i,m,n an odd permutation of 1,2,3}$$

$$\varepsilon_{imn} = 0 \quad \text{otherwise.}$$

This gives the gradient tensor components

$$\frac{\partial H_i}{\partial R_j} = \frac{I}{4\pi}\{\varepsilon_{imn}\hat{1}_m\delta_{nj}I_1 - 3[\hat{\mathbf{l}}\times(\mathbf{R}-\mathbf{R}_1)]_i\,[(R_j - R_{1j})I_2 - \hat{1}_j I_3]\} \tag{126}$$

where

$$I_2 = \int_0^{|\mathbf{R}_1-\mathbf{R}_2|} \frac{du}{\left(\sqrt{u^2 - 2\hat{\mathbf{l}}\cdot(\mathbf{R}-\mathbf{R}_1)u + |\mathbf{R}-\mathbf{R}_1|^2}\right)^5} \tag{127}$$

and

$$I_3 = \int_0^{|\mathbf{R}_1-\mathbf{R}_2|} \frac{du\,u}{\left(\sqrt{u^2 - 2\hat{\mathbf{l}}\cdot(\mathbf{R}-\mathbf{R}_1)u + |\mathbf{R}-\mathbf{R}_1|^2}\right)^5}. \tag{128}$$

Explicitly, define

$$\mathcal{J} = \frac{1}{|\mathbf{R}_1-\mathbf{R}|^2[1-(\hat{\mathbf{l}}\cdot\hat{\mathbf{u}}_1)^2]}\left[\frac{2\hat{\mathbf{l}}\cdot(\hat{\mathbf{u}}_2-\hat{\mathbf{u}}_1)}{1-(\hat{\mathbf{l}}\cdot\hat{\mathbf{u}}_1)^2} + \hat{\mathbf{l}}\cdot(\alpha_{12}^2\hat{\mathbf{u}}_2 - \hat{\mathbf{u}}_1)\right] \tag{129}$$

$$\mathcal{K} = \frac{1}{|\mathbf{R}_1-\mathbf{R}|^2} - \frac{\alpha_{12}}{|\mathbf{R}_2-\mathbf{R}|^2} - (\hat{\mathbf{l}}\cdot\hat{\mathbf{u}}_1)\mathcal{J} \tag{130}$$

with

$$\alpha_{12} = \frac{|\mathbf{R}_1-\mathbf{R}|}{|\mathbf{R}_2-\mathbf{R}|}. \tag{131}$$

Then

$$I_2 = \frac{\mathcal{J}}{3|\mathbf{R}_1-\mathbf{R}|^2} \tag{132}$$

$$I_3 = \frac{\mathcal{K}}{3|\mathbf{R}_1-\mathbf{R}|} \tag{133}$$

and the gradient tensor components can all be written in the compact form

$$\frac{\partial H_i}{\partial R_j} = \frac{I}{4\pi}[\varepsilon_{imj}\hat{\mathbf{l}}_m I_1 - (\hat{\mathbf{l}} \times \hat{\mathbf{u}}_1)_i (\hat{\mathbf{l}}_j \mathcal{K} + \hat{u}_{1j} \mathcal{J})]. \tag{134}$$

Here, it is noted that

$$\nabla \cdot \mathbf{H} = -\frac{I}{4\pi}\{(\hat{\mathbf{l}} \times \hat{\mathbf{u}}_1) \cdot \hat{\mathbf{l}}\mathcal{K} + (\hat{\mathbf{l}} \times \hat{\mathbf{u}}_1) \cdot \hat{\mathbf{u}}_1 \mathcal{J}\} \equiv 0. \tag{135}$$

GRADIENT MEASUREMENTS: HOUSING EFFECTS

The presence of a distributed current causes the undisturbed gradient tensor to be asymmetric via the relation $\nabla \times \mathbf{H} = \mathbf{J}$. However, any practical gradiometer will be housed in a container that excludes the current from the measurement volume. This will have a profound effect on the measurement, in that it may modify the magnetic field in the enclosure relative to the original field, and it forces the measured gradient tensor to be symmetric, possibly in a way that may be difficult to determine.

Joseph, et. al.,[1,2,3] have analyzed the effects of enclosures to determine the relationship between the measured field vector and gradient tensor components and those that exist in the absence of the enclosure. They have given detailed results for spherical and axisymmetric enclosures under the assumption that there are no other boundaries, and that the undisturbed current density $\mathbf{J}^0$ is uniform over the volume occupied by the enclosure.

SPHERICAL ENCLOSURE

For a spherical enclosure, the interior field has the form

$$\mathbf{H} = \mathbf{H}^0 + \mathbf{H}' \tag{136}$$

where $\mathbf{H}^0$ is the field in the absence of the enclosure, and $\mathbf{H}'$ is the distortion field, which is related to the current $\mathbf{J}^0$ via

$$\mathbf{H}' = \frac{1}{2}(\mathbf{r} \times \mathbf{J}^0) \tag{137}$$

From this expression, it is clear that the enclosure has no effect on the field at the center of the sphere. Away from the center, there is a nonzero correction term. The expression also can be used to show that the effect of the enclosure on the gradient tensor is to select the symmetric part of the tensor; that is,

$$G_{ij} = \frac{1}{2}(G_{ij}^0 + G_{ji}^0) \tag{138}$$

an expression that holds *everywhere within the enclosure.* Thus, the measured gradient tensor may be easily calculated in terms of the undistorted tensor.

AXISYMMETRIC ENCLOSURE

In the axisymmetric case, the enclosure affects the field in the following way. On the symmetry axis, the axial distortion field is zero, while the field perpendicular to (athwart) the axis has nontrivial corrections. Off the symmetry axis, both components of the field have nontrivial corrections.

For the gradient tensor, on the symmetry axis, the diagonal components are undistorted, and those involving derivatives with respect to the coordinates perpendicular to the symmetry axis are symmetrized as in the spherical case. Those components involving derivatives with respect to the axial coordinate have corrections that depend on both the ambient current density and the axial enclosure profile, and these corrections may be as large as the undisturbed gradients.

GENERAL ENCLOSURE

In the general nonsymmetric enclosure case, all the gradient tensor components have nontrivial corrections depending on the current density vector and the enclosure shape. The determination of the corrections involves the solution of the system of equations[3]

$$\mathbf{H}'(\mathbf{r}) = \oint_S dS' \frac{1}{4\pi|\mathbf{r}-\mathbf{r}'|} \hat{\mathbf{n}}' \times (\mathbf{J}_S^0 - \sigma \nabla' \phi') \tag{139}$$

$$\nabla^2 \phi' = 0 \tag{140}$$

$$\phi' \underset{\infty}{\rightarrow} 0 \tag{141}$$

and

$$\sigma \hat{\mathbf{n}} \cdot \nabla \phi' = \hat{\mathbf{n}} \cdot \mathbf{J}^0 |_S \tag{142}$$

where ϕ is the potential due to the presence of the enclosure in the ambient (uniform) current distribution, σ is the medium conductivity, and $\hat{\mathbf{n}}$ is the outward normal to the surface of the enclosure.

The computation of enclosure corrections is beyond the scope of this report. It will be limited to the case of a spherical enclosure. For this case the measured gradient tensor from the electrode-cable combination will have the form

$$G^s = \begin{pmatrix} G_{xx}^e + G_{xx}^c & \frac{1}{2}(G_{xy}^e + G_{yx}^e + G_{xy}^c + G_{yx}^c) & \frac{1}{2}(G_{xz}^e + G_{xz}^c + G_{zx}^c) \\ \frac{1}{2}(G_{xy}^e + G_{yx}^e + G_{xy}^c + G_{yx}^c) & (G_{yy}^c - G_{xx}^e) & \frac{1}{2}(G_{yz}^e + G_{yz}^c + G_{zy}^c) \\ \frac{1}{2}(G_{xz}^e + G_{xz}^c + G_{zx}^c) & \frac{1}{2}(G_{yz}^e + G_{yz}^c + G_{zy}^c) & -(G_{xx}^c + G_{yy}^c) \end{pmatrix}. \tag{143}$$

REFERENCES

1. Joseph, R. I.; Thomas, M. E.; and Allen, K. R., *Magnetic Field and Field Gradient Corrections within a Nonconducting Sensor Enclosure in a Conducting Fluid-Part I: Potential Flow*, IEEE Trans. Geosci. Rem. Sens., **GE-21**, #4, Oct 1983.

2. Joseph, R. I.; Thomas, M. E., *Magnetic Field and Field Gradient Corrections within a Nonconducting Sensor Enclosure in a Conducting Fluid-Part II: Vorticity*, IEEE Trans. Geosci. Rem. Sens., **GE-22**, #2, Mar 1984.

3. Joseph, R. I., *Magnetic Field and Field Gradient Corrections within a Nonconducting Sensor Enclosure in a Conducting Fluid-Part III: Current Exclusion Contribution for an Arbitrary Axisymmetric Enclosure*, IEEE Trans. Geosci. Rem. Sens., **GE-22**, #4, Jul 1984.

APPENDIX A

TRANSERA HIGH TECH BASIC CODES FOR REGION 1

CURRENT DENSITY CODE

```
10   SUB Jelectrode(R(*),Re(*),Db,S,Sb,I,Jay(*),Err)
20    X=R(1)
30    Y=R(2)
40    Z=R(3)
50    Xe=Re(1)
60    Ye=Re(2)
70    Ze=Re(3)
80    Dx=X-Xe
90    Dy=Y-Ye
100   IF SQR((Dx*Dx+Dy*Dy)/(X*X+Y*Y+Xe*Xe+Ye*Ye))<1.E-12 THEN
110     Jay(1)=0
120     Jay(2)=0
130     Jay(3)=0
140     GOTO 1560
150   END IF
160     !
170     !This program calculates the current density within the upper
180     !layer of a two-layer conductor, bounded above by air, due to
190     !an electrode injecting a current I into that layer.  X,Y, and
200     !Z are the coordinates (meters) of the field point in a coordi-
210     !nate system whose origin is at the surface.  Xe, Ye, and Ze are
220     !the coordinates (meters) of the electrode.  Db is the depth to
230     !the conductor-conductor  boundary below the air-conductor bound-
240     !ary.  S is the conductivity (Siemens/meter) of the upper conduct-
250     !ing layer and Sb is that for the lower layer(for Sb=0, corre-
260     !sponding to an insulating bottom, or Sb<0, a perfectly conducting
270     !bottom, alternate series expressions are used).  Jay(*) is the
280     !three-component field vector in amperes/meter^2.  Err is the size
290     !of the summand relative to the sum when summation ceases.  Note
300     !that I is positive if current enters the medium from the electrode
310     !and negative otherwise.
320     !
330   OPTION BASE 1
340   IF Sb>0 THEN
350     Q=(S-Sb)/(S+Sb)
360   ELSE
370     IF Sb=0 THEN
380       Q=1
390     ELSE
400       Q=-1
410     END IF
420   END IF
430   X2=(X-Xe)*(X-Xe)
440   Y2=(Y-Ye)*(Y-Ye)
450   R0=SQR(X2+Y2)
460   R03=R0*R0*R0
```

```
470  Rm=SQR(R0*R0+(Z-Ze)*(Z-Ze))
480  Rm3=Rm*Rm*Rm
490  Rp=SQR(R0*R0+(Z+Ze)*(Z+Ze))
500  Rp3=Rp*Rp*Rp
510  IF ABS(Q)<1 THEN
520   Smxy=1/Rm3+1/Rp3
530   Smz=(Z-Ze)/Rm3+(Z+Ze)/Rp3
540   Qn=Q
550   N=1
560   Zmm=2*N*Db-Z-Ze
570   Zpp=2*N*Db+Z+Ze
580   Zmp=2*N*Db-Z+Ze
590   Zpm=2*N*Db+Z-Ze
600   Rmm=SQR(R0*R0+Zmm*Zmm)
610   Rpp=SQR(R0*R0+Zpp*Zpp)
620   Rmp=SQR(R0*R0+Zmp*Zmp)
630   Rpm=SQR(R0*R0+Zpm*Zpm)
640   Rmm3=Rmm*Rmm*Rmm
650   Rpp3=Rpp*Rpp*Rpp
660   Rmp3=Rmp*Rmp*Rmp
670   Rpm3=Rpm*Rpm*Rpm
680   Intz=Qn*(-Zmm/Rmm3+Zpp/Rpp3-Zmp/Rmp3+Zpm/Rpm3)
690   Intxy=Qn*(1/Rmm3+1/Rpp3+1/Rmp3+1/Rpm3)
700   Smz=Smz+Intz
710   Smxy=Smxy+Intxy
720   IF N>4 THEN
730    IF ABS(Intz/Smz)<Err THEN
740     IF ABS(Intxy/Smxy)<Err THEN
750      GOTO 820
760     END IF
770    END IF
780   END IF
790   N=N+1
800   Qn=Q*Qn
810   GOTO 560
820   Jay(3)=I*Smz/4/PI
830   Jay(1)=(X-Xe)*I*Smxy/4/PI
840   Jay(2)=(Y-Ye)*I*Smxy/4/PI
850  ELSE
860   Zm=Z-Ze
870   Zp=Z+Ze
880   Smxy=0
890   Smz=0
900   Fxy=0
910   Fz=0
920   IF Q=1 THEN
930    N=1
940    CALL K0(N*PI*R0/Db,K0)
950    CALL K1(N*PI*R0/Db,K1)
960    Intxy=N*K1*(COS(N*PI*Zm/Db)+COS(N*PI*Zp/Db))
970    Intz=N*K0*(SIN(N*PI*Zm/Db)+SIN(N*PI*Zp/Db))
980    Smxy=Smxy+Intxy
```

```
990     Smz=Smz+Intz
1000     IF N>4 THEN
1010       IF ABS(Smxy)=0 THEN
1020         Fxy=1
1030       ELSE
1040         IF ABS(Intxy)/ABS(Smxy)<Err THEN
1050           Fxy=1
1060         END IF
1070       END IF
1080       IF ABS(Smz)=0 THEN
1090         Fz=1
1100       ELSE
1110         IF ABS(Intz)/ABS(Smz)<Err THEN
1120           Fz=1
1130         END IF
1140       END IF
1150       IF Fxy+Fz>1 THEN GOTO 1190
1160       N=N+1
1170       GOTO 940
1180     END IF
1190     Jay(3)=I/2/Db/Db*Smz
1200     Jfac=I/(2*PI*R0*R0*Db)*(1+PI*R0/Db*Smxy)
1210     Jay(1)=(X-Xe)*Jfac
1220     Jay(2)=(Y-Ye)*Jfac
1230   ELSE
1240     N=0
1250     CALL K0((N+.5)*PI*R0/Db,K0)
1260     CALL K1((N+.5)*PI*R0/Db,K1)
1270     Intxy=(N+.5)*K1*(COS((N+.5)*PI*Zm/Db)+COS((N+.5)*PI*Zp/Db))
1280     Intz=(N+.5)*K0*(SIN((N+.5)*PI*Zm/Db)+SIN((N+.5)*PI*Zp/Db))
1290     Smxy=Smxy+Intxy
1300     Smz=Smz+Intz
1310     IF N>4 THEN
1320       IF ABS(Smxy)=0 THEN
1330         Fxy=1
1340       ELSE
1350         IF ABS(Intxy)/ABS(Smxy)<Err THEN
1360           Fxy=1
1370         END IF
1380       END IF
1390       IF ABS(Smz)=0 THEN
1400         Fz=1
1410       ELSE
1420         IF ABS(Intz)/ABS(Smz)<Err THEN
1430           Fz=1
1440         END IF
1450       END IF
1460       IF Fxy+Fz>1 THEN GOTO 1500
1470       N=N+1
1480       GOTO 1250
1490     END IF
1500     Jay(3)=I/2/Db/Db*Smz
```

```
1510      Jfac=I/(2*R0*Db*Db)
1520      Jay(1)=(X-Xe)*Jfac*Smxy
1530      Jay(2)=(Y-Ye)*Jfac*Smxy
1540     END IF
1550   END IF
1560 SUBEND
```

ELECTRODE MAGNETIC FIELD CODE

```
10   SUB Helectrode(R(*),Re(*),Db,S,Sb,I,Aitch(*),Err)
20     X=R(1)
30     Y=R(2)
40     Z=R(3)
50     Xe=Re(1)
60     Ye=Re(2)
70     Ze=Re(3)
80     Dx=X-Xe
90     Dy=Y-Ye
100    IF SQR((Dx*Dx+Dy*Dy)/(X*X+Y*Y+Xe*Xe+Ye*Ye))<1.E-12 THEN
110      Aitch(1)=0
120      Aitch(2)=0
130      Aitch(3)=0
140      GOTO 1080
150    END IF
160      !
170      !This program calculates the magnetic field within the upper
180      !layer of a two-layer conductor, bounded above by air, due to
190      !an electrode injecting a current I into that layer.  X,Y, and
200      !Z are the coordinates (meters) of the field point in a coordi-
210      !nate system whose origin is at the surface.  Xe, Ye, and Ze are
220      !the coordinates (meters) of the electrode.  Db is the depth to
230      !the conductor-conductor  boundary below the air-conductor bound-
240      !ary.  S is the conductivity (Siemens/meter) of the upper conduct-
250      !ing layer and Sb is that for the lower layer(for Sb=0, corre-
260      !sponding to an insulating bottom, or Sb<0, a perfectly conducting
270      !bottom, alternate series expressions are used).  Aitch(*) is
280      !the three-component field vector(amperes/meter).  Err is the size
290      !of the summand relative to the sum when summation ceases.  Note
300      !that I is positive if current enters the medium from the electrode
310      !and negative otherwise.
320      !
330    OPTION BASE 1
340    IF Sb>0 THEN
350      Q=(S-Sb)/(S+Sb)
360    ELSE
370      IF Sb=0 THEN
380        Q=1
390      ELSE
400        Q=-1
410      END IF
```

```
420   END IF
430   X2=(X-Xe)*(X-Xe)
440   Y2=(Y-Ye)*(Y-Ye)
450   R0=SQR(X2+Y2)
460   R03=R0*R0*R0
470   Rp=SQR(R0*R0+(Z+Ze)*(Z+Ze))
480   R3=Rp*Rp*Rp
490   IF ABS(Q)<1 THEN
500     Sm=1-(Z+Ze)/Rp
510     Qn=Q
520     N=1
530     Zmm=2*N*Db-Z-Ze
540     Zpp=2*N*Db+Z+Ze
550     Zmp=2*N*Db-Z+Ze
560     Zpm=2*N*Db+Z-Ze
570     Rmm=SQR(R0*R0+Zmm*Zmm)
580     Rpp=SQR(R0*R0+Zpp*Zpp)
590     Rmp=SQR(R0*R0+Zmp*Zmp)
600     Rpm=SQR(R0*R0+Zpm*Zpm)
610     Int=Qn*(Zmm/Rmm-Zpp/Rpp+Zmp/Rmp-Zpm/Rpm)
620     Sm=Sm+Int
630     IF N>2 THEN
640       IF ABS(Int/Sm)<Err THEN
650         Sm=I*Sm/(4*PI*R0)
660         GOTO 1050
670       END IF
680     END IF
690     N=N+1
700     Qn=Q*Qn
710     GOTO 530
720   ELSE
730     Sm=0
740     Zm=Z-Ze
750     Zp=Z+Ze
760     Rm=SQR(R0*R0+Zm*Zm)
770     IF Q=1 THEN
780       N=1
790       CALL K1(N*PI*R0/Db,K1)
800       Int=K1*(SIN(N*PI*Zm/Db)+SIN(N*PI*Zp/Db))
810       Sm=Sm+Int
820       IF N>=2 THEN
830         IF ABS(Int)/ABS(Sm)<Err THEN 880
840       ELSE
850         N=N+1
860         GOTO 790
870       END IF
880       Sm=1-2*Z/Db+Zm/Rm+PI*R0/Db*Sm
890       Sm=I*Sm/(4*PI*R0)
900     ELSE
910       N=0
920       CALL K1((N+.5)*PI*R0/Db,K1)
930       Int=K1*(SIN((N+.5)*PI*Zm/Db)+SIN((N+.5)*PI*Zp/Db))
```

```
940        Sm=Sm+Int
950        IF N>=2 THEN
960          IF ABS(Int)/ABS(Sm)<Err THEN 1010
970        ELSE
980          N=N+1
990          GOTO 920
1000       END IF
1010       Sm=1+Zm/Rm-2*R0/Db*Sm
1020       Sm=I*Sm/(4*PI*R0)
1030     END IF
1040   END IF
1050   Aitch(1)=(Ye-Y)*Sm/R0
1060   Aitch(2)=(X-Xe)*Sm/R0
1070   Aitch(3)=0
1080 SUBEND
```

ELECTRODE MAGNETIC FIELD GRADIENT CODE

```
10   SUB Gelectrode(R(*),Re(*),Db,S,Sb,I,G(*),Err)
20     OPTION BASE 1
30     DIM H(3)
40     X=R(1)
50     Y=R(2)
60     Z=R(3)
70     Xe=Re(1)
80     Ye=Re(2)
90     Ze=Re(3)
100      !
110      !This program calculates the magnetic field gradient within the upper
120      !layer of a two-layer conductor, bounded above by air, due to
130      !an electrode injecting a current I into that layer.  X,Y, and
140      !Z are the coordinates (meters) of the field point in a coordi-
150      !nate system whose origin is at the surface.  Xe, Ye, and Ze are
160      !the coordinates (meters) of the electrode.  Db is the depth to
170      !the conductor-conductor  boundary below the air-conductor bound-
180      !ary.  S is the conductivity (Siemens/meter) of the upper conduct-
190      !ing layer and Sb is that for the lower layer(for Sb=0, corre-
200      !sponding to an insulating bottom, or Sb<0, a perfectly conducting
210      !bottom, alternate series expressions are used).  G(*) is the
220      !3x3 magnetic gradient tensor(amperes/meter^2).  Err is the size
230      !of the summand relative to the sum when summation ceases.  Note
240      !that I is positive if current enters the medium from the electrode
250      !and negative otherwise.
260      !
270    IF Sb>0 THEN
280      Q=(S-Sb)/(S+Sb)
290    ELSE
300      IF Sb=0 THEN
310        Q=1
320      ELSE
```

```
330      Q=-1
340     END IF
350   END IF
360   X2=(X-Xe)*(X-Xe)
370   Y2=(Y-Ye)*(Y-Ye)
380   Xy=(X-Xe)*(Y-Ye)
390   R0=SQR(X2+Y2)
400   R02=R0*R0
410   R03=R0*R0*R0
420   Rp=SQR(R0*R0+(Z+Ze)*(Z+Ze))
430   R3=Rp*Rp*Rp
440   IF ABS(Q)<1 THEN
450     Smtr=(Z+Ze)/R3
460     Smtz=(Z+Ze)*(Z+Ze)/R3-1/Rp
470     Qn=Q
480     N=1
490     Zmm=2*N*Db-Z-Ze
500     Zmm2=Zmm*Zmm
510     Zpp=2*N*Db+Z+Ze
520     Zpp2=Zpp*Zpp
530     Zmp=2*N*Db-Z+Ze
540     Zmp2=Zmp*Zmp
550     Zpm=2*N*Db+Z-Ze
560     Zpm2=Zpm*Zpm
570     Rmm=SQR(R0*R0+Zmm*Zmm)
580     Rmm3=Rmm*Rmm*Rmm
590     Rpp=SQR(R0*R0+Zpp*Zpp)
600     Rpp3=Rpp*Rpp*Rpp
610     Rmp=SQR(R0*R0+Zmp*Zmp)
620     Rmp3=Rmp*Rmp*Rmp
630     Rpm=SQR(R0*R0+Zpm*Zpm)
640     Rpm3=Rpm*Rpm*Rpm
650     Inttr=Qn*(-Zmm/Rmm3+Zpp/Rpp3-Zmp/Rmp3+Zpm/Rpm3)
660     Inttz=Qn*(Zmm2/Rmm3+Zpp2/Rpp3+Zmp2/Rmp3+Zpm2/Rpm3)
670     Inttz=Inttz+Qn*(-1/Rmm-1/Rpp-1/Rmp-1/Rpm)
680     Smtr=Smtr+Inttr
690     Smtz=Smtz+Inttz
700     IF N>2 THEN
710       IF ABS(Inttr/Smtr)<Err THEN
720         IF ABS(Inttz/Smtz)<Err THEN
730           Smtr=I*Smtr/(4*PI)
740           Smtz=I*Smtz/(4*PI*R0)
750           GOTO 1290
760         END IF
770       END IF
780     END IF
790     N=N+1
800     Qn=Q*Qn
810     GOTO 490
820   ELSE
830     Smtr=0
840     Smtz=0
```

```
850   Zm=Z-Ze
860   Zp=Z+Ze
870   Rm=SQR(R0*R0+Zm*Zm)
880   Rm3=Rm*Rm*Rm
890   IF Q=1 THEN
900     N=1
910     CALL K0(N*PI*R0/Db,K0)
920     Inttr=N*K0*(SIN(N*PI*Zm/Db)+SIN(N*PI*Zp/Db))
930     Smtr=Smtr+Inttr
940     CALL K1(N*PI*R0/Db,K1)
950     Inttz=N*K1*(COS(N*PI*Zm/Db)+COS(N*PI*Zp/Db))
960     Smtz=Smtz+Inttz
970     IF N>=2 THEN
980       IF ABS(Inttr)/ABS(Smtr)<Err THEN
990         IF ABS(Inttz)/ABS(Smtz)<Err THEN
1000          GOTO 1060
1010        END IF
1020      END IF
1030    END IF
1040    N=N+1
1050    GOTO 910
1060    Smtr=I*(-(1+Zm/Rm-2*Z/Db)/R02-Zm/Rm3+PI*PI/Db/Db*Smtr)/4/PI
1070    Smtz=I*(-2/Db-Zm*Zm/Rm3+1/Rm+PI*PI*R0*Smtz/Db/Db)/(4*PI*R0)
1080  ELSE
1090    N=0
1100    CALL K0((N+.5)*PI*R0/Db,K0)
1110    Inttr=(N+.5)*K0*(SIN((N+.5)*PI*Zm/Db)+SIN((N+.5)*PI*Zp/Db))
1120    Smtr=Smtr+Inttr
1130    CALL K1((N+.5)*PI*R0/Db,K1)
1140    Inttz=(N+.5)*K1*(COS((N+.5)*PI*Zm/Db)+COS((N+.5)*PI*Zp/Db))
1150    Smtz=Smtz+Inttz
1160    IF N>=2 THEN
1170      IF ABS(Inttr)/ABS(Smtr)<Err THEN
1180        IF ABS(Inttz)/ABS(Smtz)<Err THEN
1190          GOTO 1250
1200        END IF
1210      END IF
1220    END IF
1230    N=N+1
1240    GOTO 1100
1250    Smtr=-I*(Zm/Rm/R02+Zm/Rm3+2*PI*Smtr/Db/Db)/4/PI
1260    Smtz=I*(-Zm*Zm/Rm3+1/Rm-2*PI*R0*Smtz/Db/Db)/(4*PI*R0)
1270  END IF
1280 END IF
1290 CALL Helectrode(R(*),Re(*),Db,S,Sb,I,H(*),Err)
1300 Ht=(X-Xe)*H(2)/R0-(Y-Ye)*H(1)/R0
1310 IF ABS(Q)<1 THEN
1320   Smtr=Smtr-Ht/R0
1330 END IF
1340 G(1,1)=Xy*(Ht-R0*Smtr)/R03
1350 G(2,2)=-G(1,1)
1360 G(3,3)=0
```

```
1370  G(3,1)=0
1380  G(3,2)=0
1390  G(1,2)=-(X2*Ht+R0*Y2*Smtr)/R03
1400  G(2,1)=(Y2*Ht+R0*X2*Smtr)/R03
1410  G(1,3)=-(Y-Ye)*Smtz/R0
1420  G(2,3)=(X-Xe)*Smtz/R0
1430 SUBEND
```

BIOT-SAVART MAGNETIC FIELD CODE

```
10   SUB Hbiotsavrt(I,R1(*),R2(*),R(*),H(*))
20    OPTION BASE 1
30    DIM X1(3),X2(3),X12(3),L(3),U1(3),U2(3)
40      !
50      !This program calculates the magnetic field H(*) (amperes/meter)
60      !at the point R(*) (meters), due to a straight wire segment
70      !whose end points are R1(*) and R2(*) (meters), and in which
80      !the current flows from R1(*) to R2(*).
90      !
100   X1(1)=R1(1)-R(1)
110   X1(2)=R1(2)-R(2)
120   X1(3)=R1(3)-R(3)
130   X2(1)=R2(1)-R(1)
140   X2(2)=R2(2)-R(2)
150   X2(3)=R2(3)-R(3)
160   X12(1)=R2(1)-R1(1)
170   X12(2)=R2(2)-R1(2)
180   X12(3)=R2(3)-R1(3)
190   R1m=SQR(DOT(X1,X1))
200   R2m=SQR(DOT(X2,X2))
210   R12m=SQR(DOT(X12,X12))
220   MAT L= (1/R12m)*X12
230   MAT U1= (1/R1m)*X1
240   MAT U2= (1/R2m)*X2
250   N=DOT(L,U1)-DOT(L,U2)
260   D=1-DOT(L,U1)*DOT(L,U1)
270   Fac=(I*N)/(4*PI*R1m*D)
280   H(1)=L(2)*U1(3)-L(3)*U1(2)
290   H(2)=L(3)*U1(1)-L(1)*U1(3)
300   H(3)=L(1)*U1(2)-L(2)*U1(1)
310   MAT H= (Fac)*H
320  SUBEND
```

BIOT-SAVART MAGNETIC FIELD GRADIENT CODE

```
10   SUB Gbiotsavrt(I,R1(*),R2(*),R(*),G(*))
20    OPTION BASE 1
30    DIM X1(3),X2(3),X12(3),L(3),U1(3),U2(3)
```

```
40    !
50    !This program calculates the magnetic field gradient tensor
60    !G(*) (ampere/meter^2) at the point R(*) (meters), due to a
70    !straight wire segment whose end points are R1(*) and R2(*)
80    !(meters) and in which positive current I flows from R1(*)
90    !to R2(*).
100   !
110   X1(1)=R1(1)-R(1)
120   X1(2)=R1(2)-R(2)
130   X1(3)=R1(3)-R(3)
140   X2(1)=R2(1)-R(1)
150   X2(2)=R2(2)-R(2)
160   X2(3)=R2(3)-R(3)
170   X12(1)=R2(1)-R1(1)
180   X12(2)=R2(2)-R1(2)
190   X12(3)=R2(3)-R1(3)
200   R1m=SQR(DOT(X1,X1))
210   R2m=SQR(DOT(X2,X2))
220   R12m=SQR(DOT(X12,X12))
230   MAT L=(1/R12m)*X12
240   MAT U1=(1/R1m)*X1
250   MAT U2=(1/R2m)*X2
260   N=DOT(L,U1)-DOT(L,U2)
270   D=1-DOT(L,U1)*DOT(L,U1)
280   I1=-N/D/R1m/R1m
290   A12=R1m/R2m
300   I2=(-2*N/D+A12*A12*DOT(L,U2)-DOT(L,U1))/D/R1m/R1m
310   I3=1/R1m/R1m-A12/R2m/R2m-DOT(L,U1)*I2
320   Gfac=I/4/PI
330   G(1,1)=Gfac*(-L(2)*U1(3)+L(3)*U1(2))*(L(1)*I3+U1(1)*I2)
340   G(2,2)=Gfac*(-L(3)*U1(1)+L(1)*U1(3))*(L(2)*I3+U1(2)*I2)
350   G(3,3)=-G(1,1)-G(2,2)
360   G(1,2)=Gfac*(-L(3)*I1+(-L(2)*U1(3)+L(3)*U1(2))*(L(2)*I3+U1(2)*I2))
370   G(2,1)=Gfac*(L(3)*I1+(-L(3)*U1(1)+L(1)*U1(3))*(L(1)*I3+U1(1)*I2))
380   G(1,3)=Gfac*(L(2)*I1+(-L(2)*U1(3)+L(3)*U1(2))*(L(3)*I3+U1(3)*I2))
390   G(3,1)=Gfac*(-L(2)*I1+(-L(1)*U1(2)+L(2)*U1(1))*(L(1)*I3+U1(1)*I2))
400   G(2,3)=Gfac*(-L(1)*I1+(-L(3)*U1(1)+L(1)*U1(3))*(L(3)*I3+U1(3)*I2))
410   G(3,2)=Gfac*(L(1)*I1+(-L(1)*U1(2)+L(2)*U1(1))*(L(2)*I3+U1(2)*I2))
420 SUBEND
```

MODIFIED BESSEL FUNCTION CODES

```
10  SUB I0(X,I0)
20    !
30    !calculates the modified bessel function I0(x) for real x>=0
40    !
50    OPTION BASE 1
60    DIM A(9),T(9)
70    MAT A=(0)
80    MAT T=(0)
```

```
90  U=X/3.75
100  IF U<=1 THEN
110   A(1)=1
120   A(2)=3.5156229
130   A(3)=3.0899424
140   A(4)=1.2067492
150   A(5)=.2659732
160   A(6)=.0360768
170   A(7)=.0045813
180   T(1)=1
190   T(2)=U*U
200   T(3)=T(2)*T(2)
210   T(4)=T(2)*T(3)
220   T(5)=T(3)*T(3)
230   T(6)=T(2)*T(5)
240   T(7)=T(4)*T(4)
250   I0=DOT(A,T)
260  ELSE
270   A(1)=.39894228
280   A(2)=.01328592
290   A(3)=.00225319
300   A(4)=-.00157565
310   A(5)=.00916281
320   A(6)=-.02057706
330   A(7)=.02635537
340   A(8)=-.01647633
350   A(9)=.00392377
360   T(1)=1
370   T(2)=1/U
380   T(3)=T(2)*T(2)
390   T(4)=T(2)*T(3)
400   T(5)=T(3)*T(3)
410   T(6)=T(2)*T(5)
420   T(7)=T(4)*T(4)
430   T(8)=T(2)*T(7)
440   T(9)=T(5)*T(5)
450   I0=EXP(X)/SQR(X)*DOT(A,T)
460  END IF
470 SUBEND

480 SUB I1(X,I1)
490  !
500  !calculates the modified bessel function I1(x) for real x>=0
510  !
520  OPTION BASE 1
530  DIM A(9),T(9)
540  MAT A=(0)
550  MAT T=(0)
560  U=X/3.75
570  IF U<=1 THEN
580   A(1)=.5
590   A(2)=.87890594
```

```
600    A(3)=.51498869
610    A(4)=.15084934
620    A(5)=.02658733
630    A(6)=.00301532
640    A(7)=.00032411
650    T(1)=1
660    T(2)=U*U
670    T(3)=T(2)*T(2)
680    T(4)=T(2)*T(3)
690    T(5)=T(3)*T(3)
700    T(6)=T(2)*T(5)
710    T(7)=T(4)*T(4)
720    I1=X*DOT(A,T)
730   ELSE
740    A(1)=.39894228
750    A(2)=-.03988024
760    A(3)=-.00362018
770    A(4)=.00163801
780    A(5)=-.01031555
790    A(6)=.02282967
800    A(7)=-.02895312
810    A(8)=.01787654
820    A(9)=-.00420059
830    T(1)=1
840    T(2)=1/U
850    T(3)=T(2)*T(2)
860    T(4)=T(2)*T(3)
870    T(5)=T(3)*T(3)
880    T(6)=T(2)*T(5)
890    T(7)=T(4)*T(4)
900    T(8)=T(2)*T(7)
910    T(9)=T(5)*T(5)
920    I1=EXP(X)/SQR(X)*DOT(A,T)
930   END IF
940 SUBEND
950 SUB K0(X,K0)
960   !
970   !calculates the modified bessel function K0(x) for real x>=0
980   !
990   OPTION BASE 1
1000  DIM A(7),T(7)
1010  MAT A=(0)
1020  MAT T=(0)
1030  U=X/2
1040  IF U<=1 THEN
1050   A(1)=-.57721566
1060   A(2)=.42278420
1070   A(3)=.23069756
1080   A(4)=.03488590
1090   A(5)=.00262698
1100   A(6)=.00010750
1110   A(7)=.00000740
```

```
1120    T(1)=1
1130    T(2)=U*U
1140    T(3)=T(2)*T(2)
1150    T(4)=T(2)*T(3)
1160    T(5)=T(3)*T(3)
1170    T(6)=T(2)*T(5)
1180    T(7)=T(4)*T(4)
1190    CALL I0(X,I)
1200    K0=-LOG(U)*I+DOT(A,T)
1210   ELSE
1220    A(1)=1.25331414
1230    A(2)=-.07832358
1240    A(3)=.02189568
1250    A(4)=-.01062446
1260    A(5)=.00587872
1270    A(6)=-.00251540
1280    A(7)=.00053208
1290    T(1)=1
1300    T(2)=1/U
1310    T(3)=T(2)*T(2)
1320    T(4)=T(2)*T(3)
1330    T(5)=T(3)*T(3)
1340    T(6)=T(2)*T(5)
1350    T(7)=T(4)*T(4)
1360    K0=EXP(-X)/SQR(X)*DOT(A,T)
1370   END IF
1380 SUBEND
1390 SUB K1(X,K1)
1400   !
1410   !calculates the modified bessel function K1(x) for real x>=0
1420   !
1430   OPTION BASE 1
1440   DIM A(7),T(7)
1450   MAT A=(0)
1460   MAT T=(0)
1470   U=X/2
1480   IF U<=1 THEN
1490    A(1)=1
1500    A(2)=.15443144
1510    A(3)=-.67278579
1520    A(4)=-.18156897
1530    A(5)=-.01919402
1540    A(6)=-.00110404
1550    A(7)=-.00004686
1560    T(1)=1
1570    T(2)=U*U
1580    T(3)=T(2)*T(2)
1590    T(4)=T(2)*T(3)
1600    T(5)=T(3)*T(3)
1610    T(6)=T(2)*T(5)
1620    T(7)=T(4)*T(4)
1630    CALL I1(X,I)
```

```
1640    K1=LOG(U)*I+DOT(A,T)/X
1650   ELSE
1660    A(1)=1.25331414
1670    A(2)=.23498619
1680    A(3)=-.03655620
1690    A(4)=.01504268
1700    A(5)=-.00780353
1710    A(6)=.00325614
1720    A(7)=-.00068245
1730    T(1)=1
1740    T(2)=1/U
1750    T(3)=T(2)*T(2)
1760    T(4)=T(2)*T(3)
1770    T(5)=T(3)*T(3)
1780    T(6)=T(2)*T(5)
1790    T(7)=T(4)*T(4)
1800    K1=EXP(-X)/SQR(X)*DOT(A,T)
1810   END IF
1820 SUBEND
```

DISTRIBUTION

COPIES

DOD ACTIVITIES (CONUS)

ATTN DR DONALD WALTERS 1
SUPERINTENDENT
NAVAL POSTGRADUATE SCHOOL
1 UNIVERSITY CIR
MONTEREY CA 93943-5001

ATTN LISA LANGMEAD 1
COMMANDING OFFICER
NAVAL MARITIME INTELLIGENCE CENTER
4301 SUITLAND RD
WASHINGTON DC 20395-5480

COMMANDER
CARDEROCK DIVISION
NAVAL SURFACE WARFARE CENTER
BETHESDA MD 20084-5000 1

OFFICER IN CHARGE
NAVAL SURFACE WARFARE CENTER
CARDEROCK DIVISION DET
ANNAPOLIS MD 21402-1198 1

ATTN DR JOHN HOLMES 1
JOHN SCARZELLO 1
OFFICER IN CHARGE
DAHLGREN DIVISION DET WHITE OAK
NAVAL SURFACE WARFARE CENTER
10901 NEW HAMPSHIRE AVE
SILVER SPRING MD 20903-5640

COMMANDING OFFICER
DAHLGREN DIVISION
NAVAL SURFACE WARFARE CENTER
17320 DAHLGREN RD
DAHLGREN VA 22448-5100 1

COPIES

ATTN TONY BRUNO 1
COMMANDER
NAVAL UNDERSEA WARFARE CENTER
DIVISION
NEWPORT RI 02841-5047

ATTN DR TOM ROY 1
COMMANDER
COMMAND CONTROL AND OCEAN
SURVEILLANCE CENTER
53660 OCEANVIEW DR STE 317
SAN DIEGO CA 92147-5088

COMMANDER
NAVAL AIR WARFARE CENTER WEAPONS
DIVISION
1 ADMINISTRATION CIRCLE
CHINA LAKE CA 93555-6001 1

COMMANDING OFFICER
NAVAL RESEARCH LABORATORY
4555 OVERLOOK DR
WASHINGTON DC 20375-5320 1

ATTN DR ED MOZLEY 1
WILL AVERA 1
DIRECTOR
NAVAL RESEARCH LABORATORY DET
STENNIS SPACE CENTER MS 39529-5004

DIRECTOR
ADVANCED RESEARCH PROJECTS AGENCY
1400 WILSON BLVD
ARLINGTON VA 22209 1

DEFENSE TECHNICAL INFORMATION CTR
CAMERON STATION
ALEXANDRIA VA 22304-6145 12

DISTRIBUTION (CONTINUED)

	COPIES
NON-DOD ACTIVITIES (CONUS)	
ATTN GIFT AND EXCHANGE DIVISION LIBRARY OF CONGRESS WASHINGTON DC 20540	4
THE CNA CORPORATION PO BOX 16268 ALEXANDRIA VA 22302-0268	1
INTERNAL	
CODE 0543 (MSC)	5
CODE 10 (SKINNER)	1
CODE 110 (KEKELIS)	1
CODE 110B (WYNN)	6
CODE E29L (TECHNICAL LIBRARY)	4